SECURITY CLASSIFICATION OF THIS PAGE

REPORT DOCUMENTATION PAGE		Form Approved OMB No. 0704-0188

1a. REPORT SECURITY CLASSIFICATION UNCLASSIFIED		1b. RESTRICTIVE MARKINGS NONE

2a. SECURITY CLASS...

AD-A217 709

LE
R(S)

3. DISTRIBUTION / AVAILABILITY OF REPORT
APPROVED FOR PUBLIC RELEASE;
DISTRIBUTION UNLIMITED.

5. MONITORING ORGANIZATION REPORT NUMBER(S)
AFIT/CI/CIA- 89-036

6a. NAME OF PERFORMING ORGANIZATION AFIT STUDENT AT SAINT LOUIS UNIVERSITY	6b. OFFICE SYMBOL (If applicable)	7a. NAME OF MONITORING ORGANIZATION AFIT/CIA

6c. ADDRESS (City, State, and ZIP Code)	7b. ADDRESS (City, State, and ZIP Code) Wright-Patterson AFB OH 45433-6583

8a. NAME OF FUNDING / SPONSORING ORGANIZATION	8b. OFFICE SYMBOL (If applicable)	9. PROCUREMENT INSTRUMENT IDENTIFICATION NUMBER

8c. ADDRESS (City, State, and ZIP Code)

10. SOURCE OF FUNDING NUMBERS

PROGRAM ELEMENT NO.	PROJECT NO.	TASK NO.	WORK UNIT ACCESSION NO.

11. TITLE (Include Security Classification) (UNCLASSIFIED)
Multiple Versus Single Scattering of Terrestrial Infrared Longwave Radiation in an Aerosol-Laden Planetary Boundary Layer

12. PERSONAL AUTHOR(S)
Spencer Raymond Chapman

13a. TYPE OF REPORT THESIS/DISSERTATION	13b. TIME COVERED FROM _____ TO _____	14. DATE OF REPORT (Year, Month, Day) 1989	15. PAGE COUNT 100

16. SUPPLEMENTARY NOTATION APPROVED FOR PUBLIC RELEASE IAW AFR 190-1
ERNEST A. HAYGOOD, 1st Lt, USAF
Executive Officer, Civilian Institution Programs

17.	COSATI CODES		18. SUBJECT TERMS (Continue on reverse if necessary and identify by block number)
FIELD	GROUP	SUB-GROUP	

19. ABSTRACT (Continue on reverse if necessary and identify by block number)

90 02 01 046

20. DISTRIBUTION / AVAILABILITY OF ABSTRACT ☒ UNCLASSIFIED/UNLIMITED ☐ SAME AS RPT. ☐ DTIC USERS	21. ABSTRACT SECURITY CLASSIFICATION UNCLASSIFIED	
22a. NAME OF RESPONSIBLE INDIVIDUAL ERNEST A. HAYGOOD, 1st Lt, USAF	22b. TELEPHONE (Include Area Code) (513) 255-2259	22c. OFFICE SYMBOL AFIT/CI

DD Form 1473, JUN 86   Previous editions are obsolete.   SECURITY CLASSIFICATION OF THIS PAGE

AFIT/CI "OVERPRINT"

MULTIPLE VS SINGLE SCATTERING OF TERRESTRIAL

INFRARED LONGWAVE RADIATION IN AN

AEROSOL-LADEN PLANETARY BOUNDARY LAYER

Spencer Raymond Chapman, B.S.
Capt., USAF
Page Count: 100

A Thesis Presented to the Faculty of the Graduate School
of Saint Louis University in Partial Fulfillment of
the Requirements for the Degree of
Master of Science (Research)

1989

ABSTRACT

This thesis examines the quantitative difference between multiply and singly scattered infrared terrestrial radiation in an aerosol-laden planetary boundary layer (PBL). The total net (scattering plus emission) flux densities are calculated at 11 levels for each scattering process over a spectral range of 350 cm^{-1} to 2000 cm^{-1} at 50 cm^{-1} intervals. The model PBL is a summertime mid-latitude urban structure from LOWTRAN 7. The study prototype incorporates an inversion located at 2.00 km above a surface whose elevation is at sea level with a visual range of 4.0 km. The visual range and extinction coefficients decrease with height to minimums located just below the inversion to simulate a differentially mixed aerosol-laden PBL.

Results show that a pronounced total downward directed net flux develops in the presence of aerosol particles in the water vapor absorption band between 1200 cm^{-1} to 2000 cm^{-1}. This negative total flux is 44 times larger then the singly scattered flux densities. It appears that a synergistic relationship between absorption/emission and multiple scattering among the radiatively active gases and the aerosols is established.

In the water vapor window region of the infrared spectrum (830 cm^{-1} to 1250 cm^{-1}), thermal emission from the surface is able to penetrate to the top of the urban PBL. Here the difference between multiple and single scattering is reduced but mul-

tiple scattering is still numerically superior ranging from 0.02 to 1.02 times the single scattered flux densities.

REFERENCES

JOURNAL ARTICLES

Ackerman, T.P., K. Liou, and C.B. Leovy, 1975: Infrared Radiative Transfer in Polluted Atmospheres. *J. Appl. Meteor.*, *15*, 28-35.

Arking, A., and K. Grossman, 1972: The Influence of Line Shape and Band Structure on Temperatures in Planetary Atmospheres. *J. Atmos. Sci.*, *29*, 937-949.

Coakley, Jr., J.A., and R.D. Cess, 1982: The Effect of Tropospheric Aerosols on the Earth's Radiation Budget: A Parameterization for Climate Models. *J. Atmos. Sci.*, *40*, 116-138.

Dave, J.V., 1981: Transfer of Visible Radiation in the Atmosphere. *Atmos. Env.*, *15*, 1805-1820.

Hanel, G., 1976: The Properties of Atmospheric Aerosol Particles as Functions of the Relative Humidity at Thermodynamic Equilibrium with the Surrounding Moist Air. *Advances in Geophysics*, *19*, 73-188.

Hanel, G., 1972: Computation of the Extinction of Visible Radiation by Atmospheric Aerosols Particles as a Function of the Relative Humidity, Based upon Measured Properties. *Aerosol Sci.*, *3*, 377-386.

Hansen, J.E., 1969: Exact and Approximate Solutions for Multiple Scattering by Clouds and Hazy Planetary Atmospheres. *J. Atmos. Sci.*, *26*, 478-487.

Hansen, J.E., and L.D. Travis, 1974: Light Scattering in Planetary Atmospheres. *Space Sci. Rev.*, *16*, 527-610.

Hansen, J.E., A.A. Lacis, P. Lee, and W.-C. Wang, 1980: Climatic Effects of Atmospheric Aerosol. Aerosols: Anthropogenic and Natural Sources and Transport. *Ann. N.Y. Acad. Sci.*, *383*, 575-587.

Joseph, J.H., W.J. Wiscombe, and J.A. Weinman, 1976: The Delta-Eddington Approximation for Radiative Flux Transfer. *J. Atmos. Sci.*, *33*, 2452-2459.

Liou, K., 1973: A Numerical Experiment on Chandrasekhar's Discrete- ordinate Method for Radiative Transfer: Application to Cloudy and Hazy Atmospheres. *J. Atmos. Sci.*, *30*,

1303-1326.

Meador, W.E., and W.R. Weavor, 1979: Two-Stream Approximations to Radiative Transfer in Planetary Atmospheres: A Unified Description of Existing Models and a New Improvement. *J. Atmos. Sci.*, *37*, 630-643.

Nilsson, B., 1979: Meteorological Influence on Aerosol Extinction in the 0.2µm - 40µm Wavelength Range. *Applied Optics*, *18*, 3457-3473.

Schuster, A., 1905: Radiation Through a Foggy Atmosphere. *Ap. J. Optics*, *21*, 1-22.

Schwarzschild, K., 1906: On the Equilibrium of the Sun's Atmosphere. *Nachr. Gesell. Wiss. Gottingen, Math.-Phys. Kl.*, *195*, 41-53.

Shettle, E.P., and J.A. Weinman, 1970: The Transfer of Solar Irradiance Through Inhomogeneous Turbid Atmospheres Evaluated by Eddington's Approximation. *J. Atmos. Sci.*, *27*, 1048-1055.

Venkatram, A., and R. Viskanta, 1977: Radiative Effects of Elevated Pollutant Layers. *J. Appl. Meteor.*, *16*, 1256-1272.

Viskanta, R., R.W. Bergstrom, and R.O. Johnson 1977: Radiative Transfer in a Polluted Urban Planetary Boundary Layer. *J. Atmos. Sci.*, *34*, 1091-1103.

Wang, W., and G.A. Domoto, 1974: The Radiative Effect of Aerosols in the Earth's Atmosphere. *J. Appl. Meteor.*, *13*, 521-534.

Welch, R. and W. Zdunkowski, 1976: A Radiation Model of the Polluted Atmospheric Boundary Layer. *J. Atmos. Sci.*, *33*, 2170-2184.

Wiscombe, W.J., 1983: Atmospheric Radiation: 1975-1983. *Reviews of Geophysics and Space Physics*, *21*, 977-1021.

Wiscombe, W.J., and J.W. Evans, 1977: Exponential-Sum Fitting of Radiative Transmission. *J. Comput. Phys.*, *24*, 416-444.

Wiscombe, W.J., and G.W. Grams, 1976: The Backscattered Fraction in Two-Stream Approximations. *J. Atmos. Sci.*, *33*, 2440-2451.

BOOKS

Chandrasekhar, S., 1960: *Radiative Transfer*. Dover Publications, Inc., 393 pp.

Goody, R.M., 1964: *Atmospheric Radiation*. Oxford at the Claredon Press, 436 pp.

Liou, K., 1980: *An Introduction to Atmospheric Radiation*. Academic Press, Inc., 392 pp.

McCartney, E.J., 1976: *Optics of the Atmosphere*. John Wiley & Sons, 437 pp.

Paltridge, G.W., and C.M.R. Platt, 1976: *Radiative Processes in Meteorology and Climatology*. American Elsevier Publishing Company, Inc., 319 pp.

Press, W.H., B.P. Flannery, S.A. Teukolsky, and W.T. Vetterling, 1986: *Numerical Recipes The Art of Scientific Computing*. Cambridge University Press, 818 pp.

van de Hulst, H.C., 1957: *Light Scattering by Small Particles*. Dover Publications, Inc., 446 pp.

Wallace, J.M., and P.V. Hobbs, 1977: *Atmospheric Science An Introductory Survey*. Academic Press, Inc., 476 pp.

SPECIAL PUBLICATIONS and COMMUNICATIONS

Elterman, L., 1970: Vertical Attenuation Model with Eight Surface Meteorological Ranges 2 to 13 km. *Air Force Cambridge Research Laboratory*, *AFCRL-70-0200*, Air Force Cambridge Research Laboratory, Cambridge, Massachusetts.

Elterman, L., 1968: UV, Visible, and IR Attenuation for Altitudes to 50 km. *Air Force Cambridge Research Laboratory*, *AFCRL-68-0153*, Air Force Cambridge Research Laboratory, Cambridge, Massachusetts.

Isaacs, R.G., W.C-. Wang, R.D. Worsham, and S. Goldenberg, 1986: Multiple Scattering Treatment for Use in the LOWTRAN and Fascode Models. *Air Force Geophysics Laboratory*, *AFGL-TR-86-0073*, Air Force Geophysics Laboratory and Atmospheric and Environmental Research, Inc., Cambridge, Massachusetts.

Kneizys, F.X., E.P. Shettle, W.O. Gallery, J.H. Chetwynd Jr., L.W. Abreu, J.E.A. Selby, S.A. Clough, and R.W. Fenn, 1983: Atmospheric Transmittance/Radiance: Computer Code LOWTRAN 6. *Air Force Geophysics Laboratory*, *AFGL-TR-83-0187*, Air Force Geophysics Laboratory, Optical Physics

Division, Hanscom AFB, Massachusetts.

Lenoble, J., ed., 1977: Standard Procedures to Compute Atmospheric Radiative Transfer in a Scattering Atmosphere. *IAMAP*, NCAR, Boulder, Colorado.

McClatchey, R.A., R.W. Fenn, J.E.A. Selby, F.E. Volz, and J.S. Garing, 1972: Optical Properties of the Atmosphere (Third Edition). *Air Force Cambridge Research Laboratory*, *AFCRL-72-0497*, Air Force Cambridge Research Laboratory, Hanscom Field, Massachusetts.

Pallmann, A.J., 1988: Thesis Guidance Meetings, 1988-1989. *Private Communication* St. Louis University, St Louis, Missouri.

Shettle, E.P., and R.W. Fenn, 1979: Models for the Aerosols of the Lower Atmosphere and the Effects of Humididty Variations on Their Optical Properties. *Air Force Geophysics Laboratory*, *AFGL-TR-79-0214*, Optical Physics Division, Air Force Geophysics Laboratory, Hanscom AFB, Massachusetts.

Viskanta, R., and T.L. Weirich, 1979: Effects of Pollutants and Urban Parameters on Atmospheric Dispersion and Temperature. *Environmental Sciences Research Laboratory*, *EPA-600/4-79-012*, U.S. Environmental Protection Agency; Research Triangle Park, North Carolina.

Wiscombe, W.J., 1977: The Delta-Eddington Approximation for a Vertically Inhomogeneous Atmosphere. *NCAR Technical Note*, *NCAR/TN-121*, Atmospheric Analysis and Prediction Division National Center for Atmospheric Research; Boulder, Colorado.

MULTIPLE VS SINGLE SCATTERING OF TERRESTRIAL

INFRARED LONGWAVE RADIATION IN AN

AEROSOL-LADEN PLANETARY BOUNDARY LAYER

Spencer Raymond Chapman, B.S.
Capt., USAF
Page Count: 100

A Thesis Presented to the Faculty of the Graduate School
of Saint Louis University in Partial Fulfillment of
the Requirements for the Degree of
Master of Science (Research)

1989

ABSTRACT

This thesis examines the quantitative difference between multiply and singly scattered infrared terrestrial radiation in an aerosol-laden planetary boundary layer (PBL). The total net (scattering plus emission) flux densities are calculated at 11 levels for each scattering process over a spectral range of 350 cm^{-1} to 2000 cm^{-1} at 50 cm^{-1} intervals. The model PBL is a summertime mid-latitude urban structure from LOWTRAN 7. The study prototype incorporates an inversion located at 2.00 km above a surface whose elevation is at sea level with a visual range of 4.0 km. The visual range and extinction coefficients decrease with height to minimums located just below the inversion to simulate a differentially mixed aerosol-laden PBL.

Results show that a pronounced total downward directed net flux develops in the presence of aerosol particles in the water vapor absorption band between 1200 cm^{-1} to 2000 cm^{-1}. This negative total flux is 44 times larger then the singly scattered flux densities. It appears that a synergistic relationship between absorption/emission and multiple scattering among the radiatively active gases and the aerosols is established.

In the water vapor window region of the infrared spectrum (830 cm^{-1} to 1250 cm^{-1}), thermal emission from the surface is able to penetrate to the top of the urban PBL. Here the difference between multiple and single scattering is reduced but mul-

tiple scattering is still numerically superior ranging from 0.02 to 1.02 times the single scattered flux densities.

REFERENCES

JOURNAL ARTICLES

Ackerman, T.P., K. Liou, and C.B. Leovy, 1975: Infrared Radiative Transfer in Polluted Atmospheres. *J. Appl. Meteor.*, *15*, 28-35.

Arking, A., and K. Grossman, 1972: The Influence of Line Shape and Band Structure on Temperatures in Planetary Atmospheres. *J. Atmos. Sci.*, *29*, 937-949.

Coakley, Jr., J.A., and R.D. Cess, 1982: The Effect of Tropospheric Aerosols on the Earth's Radiation Budget: A Parameterization for Climate Models. *J. Atmos. Sci.*, *40*, 116-138.

Dave, J.V., 1981: Transfer of Visible Radiation in the Atmosphere. *Atmos. Env.*, *15*, 1805-1820.

Hanel, G., 1976: The Properties of Atmospheric Aerosol Particles as Functions of the Relative Humidity at Thermodynamic Equilibium with the Surrounding Moist Air. *Advances in Geophysics*, *19*, 73-188.

Hanel, G., 1972: Computation of the Extinction of Visible Radiation by Atmospheric Aerosols Particles as a Function of the Relative Humidity, Based upon Measured Properties. *Aerosol Sci.*, *3*, 377-386.

Hansen, J.E., 1969: Exact and Approximate Solutions for Multiple Scattering by Clouds and Hazy Planetary Atmospheres. *J. Atmos. Sci.*, *26*, 478-487.

Hansen, J.E., and L.D. Travis, 1974: Light Scattering in Planetary Atmospheres. *Space Sci. Rev.*, *16*, 527-610.

Hansen, J.E., A.A. Lacis, P. Lee, and W.-C. Wang, 1980: Climatic Effects of Atmospheric Aerosol. Aerosols: Anthropogenic and Natural Sources and Transport. *Ann. N.Y. Acad. Sci.*, *383*, 575-587.

Joseph, J.H., W.J. Wiscombe, and J.A. Weinman, 1976: The Delta-Eddington Approximation for Radiative Flux Transfer. *J. Atmos. Sci.*, *33*, 2452-2459.

Liou, K., 1973: A Numerical Experiment on Chandrasekhar's Discrete- ordinate Method for Radiative Transfer: Application to Cloudy and Hazy Atmospheres. *J. Atmos. Sci.*, *30*,

1303-1326.

Meador, W.E., and W.R. Weavor, 1979: Two-Stream Approximations to Radiative Transfer in Planetary Atmospheres: A Unified Description of Existing Models and a New Improvement. *J. Atmos. Sci.*, *37*, 630-643.

Nilsson, B., 1979: Meteorological Influence on Aerosol Extinction in the 0.2μm - 40μm Wavelength Range. *Applied Optics*, *18*, 3457-3473.

Schuster, A., 1905: Radiation Through a Foggy Atmosphere. *Ap. J. Optics*, *21*, 1-22.

Schwarzschild, K., 1906: On the Equilibrium of the Sun's Atmosphere. *Nachr. Gesell. Wiss. Gottingen, Math.-Phys. Kl.*, *195*, 41-53.

Shettle, E.P., and J.A. Weinman, 1970: The Transfer of Solar Irradiance Through Inhomogeneous Turbid Atmospheres Evaluated by Eddington's Approximation. *J. Atmos. Sci.*, *27*, 1048-1055.

Venkatram, A., and R. Viskanta, 1977: Radiative Effects of Elevated Pollutant Layers. *J. Appl. Meteor.*, *16*, 1256-1272.

Viskanta, R., R.W. Bergstrom, and R.O. Johnson 1977: Radiative Transfer in a Polluted Urban Planetary Boundary Layer. *J. Atmos. Sci.*, *34*, 1091-1103.

Wang, W., and G.A. Domoto, 1974: The Radiative Effect of Aerosols in the Earth's Atmosphere. *J. Appl. Meteor.*, *13*, 521-534.

Welch, R. and W. Zdunkowski, 1976: A Radiation Model of the Polluted Atmospheric Boundary Layer. *J. Atmos. Sci.*, *33*, 2170-2184.

Wiscombe, W.J., 1983: Atmospheric Radiation: 1975-1983. *Reviews of Geophysics and Space Physics*, *21*, 977-1021.

Wiscombe, W.J., and J.W. Evans, 1977: Exponential-Sum Fitting of Radiative Transmission. *J. Comput. Phys.*, *24*, 416-444.

Wiscombe, W.J., and G.W. Grams, 1976: The Backscattered Fraction in Two-Stream Approximations. *J. Atmos. Sci.*, *33*, 2440-2451.

BOOKS

Chandrasekhar, S., 1960: *Radiative Transfer*. Dover Publications, Inc., 393 pp.

Goody, R.M., 1964: *Atmospheric Radiation*. Oxford at the Claredon Press, 436 pp.

Liou, K., 1980: *An Introduction to Atmospheric Radiation*. Academic Press, Inc., 392 pp.

McCartney, E.J., 1976: *Optics of the Atmosphere*. John Wiley & Sons, 437 pp.

Paltridge, G.W., and C.M.R. Platt, 1976: *Radiative Processes in Meteorology and Climatology*. American Elsevier Publishing Company, Inc., 319 pp.

Press, W.H., B.P. Flannery, S.A. Teukolsky, and W.T. Vetterling, 1986: *Numerical Recipes The Art of Scientific Computing*. Cambridge University Press, 818 pp.

van de Hulst, H.C., 1957: *Light Scattering by Small Particles*. Dover Publications, Inc., 446 pp.

Wallace, J.M., and P.V. Hobbs, 1977: *Atmospheric Science An Introductory Survey*. Academic Press, Inc., 476 pp.

SPECIAL PUBLICATIONS and COMMUNICATIONS

Elterman, L., 1970: Vertical Attenuation Model with Eight Surface Meteorological Ranges 2 to 13 km. *Air Force Cambridge Research Laboratory*, AFCRL-70-0200, Air Force Cambridge Research Laboratory, Cambridge, Massachusetts.

Elterman, L., 1968: UV, Visible, and IR Attenuation for Altitudes to 50 km. *Air Force Cambridge Research Laboratory*, AFCRL-68-0153, Air Force Cambridge Research Laboratory, Cambridge, Massachusetts.

Isaacs, R.G., W.C-. Wang, R.D. Worsham, and S. Goldenberg, 1986: Multiple Scattering Treatment for Use in the LOWTRAN and Fascode Models. *Air Force Geophysics Laboratory*, AFGL-TR-86-0073, Air Force Geophysics Laboratory and Atmospheric and Environmental Research, Inc., Cambridge, Massachusetts.

Kneizys, F.X., E.P. Shettle, W.O. Gallery, J.H. Chetwynd Jr., L.W. Abreu, J.E.A. Selby, S.A. Clough, and R.W. Fenn, 1983: Atmospheric Transmittance/Radiance: Computer Code LOWTRAN 6. *Air Force Geophysics Laboratory*, AFGL-TR-83-0187, Air Force Geophysics Laboratory, Optical Physics

Division, Hanscom AFB, Massachusetts.

Lenoble, J., ed., 1977: Standard Procedures to Compute Atmospheric Radiative Transfer in a Scattering Atmosphere. *IAMAP*, NCAR, Boulder, Colorado.

McClatchey, R.A., R.W. Fenn, J.E.A. Selby, F.E. Volz, and J.S. Garing, 1972: Optical Properties of the Atmosphere (Third Edition). *Air Force Cambridge Research Laboratory*, *AFCRL-72-0497*, Air Force Cambridge Research Laboratory, Hanscom Field, Massachusetts.

Pallmann, A.J., 1988: Thesis Guidance Meetings, 1988-1989. *Private Communication* St. Louis University, St Louis, Missouri.

Shettle, E.P., and R.W. Fenn, 1979: Models for the Aerosols of the Lower Atmosphere and the Effects of Humididty Variations on Their Optical Properties. *Air Force Geophysics Laboratory*, *AFGL-TR-79-0214*, Optical Physics Division, Air Force Geophysics Laboratory, Hanscom AFB, Massachusetts.

Viskanta, R., and T.L. Weirich, 1979: Effects of Pollutants and Urban Parameters on Atmospheric Dispersion and Temperature. *Environmental Sciences Research Laboratory*, *EPA-600/4-79-012*, U.S. Environmental Protection Agency; Research Triangle Park, North Carolina.

Wiscombe, W.J., 1977: The Delta-Eddington Approximation for a Vertically Inhomogeneous Atmosphere. *NCAR Technical Note*, *NCAR/TN-121*, Atmospheric Analysis and Prediction Division National Center for Atmospheric Research; Boulder, Colorado.

MULTIPLE VS SINGLE SCATTERING OF TERRESTRIAL

INFRARED LONGWAVE RADIATION IN AN

AEROSOL-LADEN PLANETARY BOUNDARY LAYER

Spencer Raymond Chapman, B.S.

A Digest Presented to the Faculty of the Graduate School
of Saint Louis University in Partial Fulfillment of
the Requirements for the Degree of
Master of Science (Research)

1989

This thesis examines the quantitative difference between multiply and singly scattered infrared terrestrial radiation in an aerosol-laden planetary boundary layer (PBL). The total net (scattering plus emission) flux densities are calculated at 11 levels for each scattering process over a spectral range of 350 cm^{-1} to 2000 cm^{-1} at 50 cm^{-1} intervals. The model PBL is a summertime mid-latitude urban structure from LOWTRAN 7. The study prototype incorporates an inversion located at 2.00 km above a surface whose elevation is at sea level with a visual range of 4.0 km. The visual range and extinction coefficients decrease with height to minimums located just below the inversion to simulate a differentially mixed aerosol-laden PBL.

Results show that a pronounced total downward directed net flux develops in the presence of aerosol particles in the water vapor absorption band between 1200 cm^{-1} to 2000 cm^{-1}. This negative total flux is 44 times larger then the singly scattered flux densities. It appears that a synergistic relationship between absorption/emission and multiple scattering among the radiatively active gases and the aerosols is established.

In the water vapor window region of the infrared spectrum (830 cm^{-1} to 1250 cm^{-1}), thermal emission from the surface is able to penetrate to the top of the urban PBL. Here the difference between multiple and single scattering is reduced but mul-

tiple scattering is still numerically superior ranging from 0.02 to 1.02 times the single scattered flux densities.

It is concluded that for the total terrestrial infrared domain multiple scattering above and beyond single scattering must be considered. Furthermore, multiple scattering in that domain leads to a coupling between the redirection of photons with increased gaseous and particulate absorption and emission at the respective layer temperature.

MULTIPLE VS SINGLE SCATTERING OF TERRESTRIAL

INFRARED LONGWAVE RADIATION IN AN

AEROSOL-LADEN PLANETARY BOUNDARY LAYER

Spencer Raymond Chapman, B.S.

A Thesis Presented to the Faculty of the Graduate School
of Saint Louis University in Partial Fulfillment of
the Requirements for the Degree of
Master of Science (Research)

1989

COMMITTEE IN CHARGE OF CANDIDANCY:

Professor Albert J. Pallmann,
        Chairperson and Advisor

Professor Gandikota Venkata Rao

Assistant Professor Lawrence Coy

ACKNOWLEDGEMENTS

TABLE OF CONTENTS

LIST OF TABLES

1.0   INTRODUCTION

1.1   Overview

Historically, the development of modeling radiative transfer in the atmosphere can be characterized as a gradual increase in complexity. Most early endeavors were concerned exclusively with short wave radiation and the phenomenon of scattering by molecules. The field began to expand in tandem with quantum mechanics and scattering theory. These branches of physics allowed investigators to include the effects of both scattering and absorption by a multitude of larger particles found in the atmosphere. But, even this advance kept the interaction of electromagnetic radiation with particles a purely "local" phenomenon concerned only with the individual particles reemissions and single scattering interplay. Stymied by such constraints the true nature of aerosol scattering within the planetary atmosphere can not be fully appreciated. In order to more completely address the question of aerosol scattering and absorption, investigations must include the effects of multiple scattering and expand the electromagnetic spectrum to include the thermal planetary domain.

1

1.2 Definition of the Research Problem

I propose to explore the question of how quantitatively significant is multiple scattering within the thermal long wave domain above and beyond single scattering in an aerosol laden boundary layer. Several cases will be investigated to determine the significance, if any, of the presence of particulate aerosol matter for infrared multiple scattering. Physically, multiple scattering on aerosol particles increases the path length that a photon will travel, thus increasing the probability of the photon interacting with all the constituents in the layers under consideration. A comparative examination of single scattering versus multiple scattering in several scenarios should allow insight to be gained into the importance of each condition as it pertains to a single control case. In addition, the inclusion of the intrinsic infrared radiative transfer from the surface boundaries and atmospheric layers, previously not included in most studies, will be more realistic when surveying the upward and downward fluxes.

1.3 Research Objectives

My topical research objective is to compare, by juxtaposition, the quantitative difference between multiply (higher order) and singly (first order) scattered infrared terrestrial flux densities in an aerosol-laden boundary layer. This will render an assessment about the significance, if any, of aerosol scattering in the longwave domain near the earth's surface.

One methodological research objective is related to my primary goal. This objective is the testing (verification and validation) and implementation of a computer code capable of simulating multiple scattering. To reach this objective, a complete restructuring of the delta-Eddington code, as presented by Wiscombe (1977) to solve for solar flux densities, to a code which is capable of producing multiply scattered infrared fluxes will be undertaken.

2.0 REVIEW OF PERTINENT LITERATURE

2.1 Infrared Radiative Effects of Aerosols

There are important reasons for pursuing aerosol radiation studies. Some of these are: 1) reduced insolation to the tropo-sphere, 2) the addition of anthropogenic soot, with its high absorption capability, to the atmosphere on a truly global scale, 3) global climate models lack any aerosol influence in their radiation parameterizations, and 4) aerosol pollution of all sorts substantially alters the urban boundary layer through radiative-dynamic interactions. Excellent reviews by McCartney (1976) and Wiscombe (1983) chronicle the study of the radiative effects of aerosols. However, it is the last reason which is the impetus for investigations of the infrared effect of aero-sols within planetary boundary layers (PBL). Viskanta and Weir-ich (1979) drew the following conclusions about the effects of aerosols in the PBL. 1) Radiatively participating aerosols in the urban environment generally give rise to cooling of the ground and warming of the PBL. Whether there is a net cooling or warming of the earth-PBL system depends upon the surface albedo, the radiation absorption, scattering characteristics of the aerosol, aerosol loading, and the vertical distribution and zenith angle (latitude, season and time of day). 2) Radiatively active gaseous pollutants alter the local energy balance and through it modify the vertical temperature structure,

4

stability, and heat fluxes at the ground.

In the early 1970's environmental concerns prompted an interest in the effects of gaseous and particulate pollutants on the radiation budget of the earth-atmosphere system on both global and regional scales. The regional studies have generally been concerned with modeling polluted urban boundary layers, and considering the effect of increased aerosol loading on the net radiative flux in the PBL. The scattering and absorption of visible (shortwave) radiant energy has been treated quite accurately by many investigators to include Welch and Zdun-kowski (1976), Viskanta et al. (1977), Coakley and Cess for climate models (1982), and Dave (1981).

Treatment of infrared radiative transfer in the PBL, how-ever, has been considerably less comprehensive and complete. Wang and Domoto (1974) were one of the first investigators to employ a modified two-stream approximation to compute the transfer of infrared radiation in a finite inhomogeneous, tur-bid atmosphere. Ackerman, Liou, and Leovy (1975) used a four stream, multi-layered radiative transfer model to treat the transfer of infrared radiation in the atmosphere containing both scatterers and absorbers. They concluded that aerosols produce insignificant influences on temperature structures in bands which exhibit strong gaseous absorption, but their effects are of considerable importance in the window region. They also found for a typical case with a low lying inversion at about 1.0 km and a uniform aerosol concentration below that

cooling in this layer can be on the order of 5°K or 10°K per day and that the aerosol effects in the infrared may influence the strength and positions of inversions.

2.2 Infrared Multiple Scattering Methodologies

Radiative transfer theory provides the mathematical description of the interaction between both external (incident solar) and internal (emitted thermal) sources of electromagnetic radiation and the radiatively active atmospheric constituents of gases and particulates. The solution to the radiative transfer equation for a scattering atmosphere (Chandrasekhar, 1960; Goody, 1964; Liou, 1980) generally require a numerical solution because of the integro-differential equations involved and that the "exact solutions" are very limited in scope of applications. So much computer time would be required to solve these exact solutions that it would be impractical to use the methods routinely. However, the "exact solutions" they could be used as a check for approximate numerical methods. Survey papers by Lenoble (1977) and Hansen et al (1974) discuss the various multiple scattering routines both exact and approximate. However, explicit mention of a routine specifically addressing infrared radiative transfer is not present. The comment is only made that a thermal term may be added to the regular radiative transfer equation to account for the diffuse component of internally generated thermal radiation.

The most commonly used numerical solution tc the radiative transfer equation is the two-stream approximation. In general, the two-stream approach is a method of representing the diffuse radiation field in two streams in one-dimensional radiation transfer problems. The approximation proposed by Schuster (1905) and Schwarzschild (1906) is to assume that the intensity in the positive direction is isotropic and that in the negative direction the intensity has a different value but is also isotropic. Meador and Weavor (1979) provide a compendium of two-stream methods and observed that all existing two-stream approximations can be represented by identical forms of coupled differential equations if the radiation intensity is replaced by integrals of the intensity over hemispheres. The two-stream methods avoid the complex and lengthy computer procedures necessary for numerical solutions of the differential equations while yielding closed-form analytical results that are relatively easy to interpret.

Shettle and Weinmann (1970) used an Eddington approximation (a form of the two-stream method) to calculate the diffuse solar flux densities in models of homogeneous turbid layers. In their paper they suggested that the infrared domain may be breached by adding to the radiative transfer equation an appropriate term to represent the thermal emission from layers under scrutiny. The same information is provided by Liou (1980). However, neither paper derives explicitly the solution to such an addition to the radiative transfer equation.

Joseph and Wiscombe (1976) identified a problem with the Eddington approximation in the presence of anisotropic scattering particles. Typically, the scattering of light in planetary atmospheres is in most cases characterized by a significantly anisotropic phase function (scattering diagram) since the presence of even a small number of haze or cloud particles results in a forward elongation of the scattered radiation field intensity. They overcame this problem using a delta function to effectively truncate the forward diffraction peak produced by the asymmetric scattering pattern of aerosol particles. While this method expanded the Eddington technique to anisotropic scattering conditions, it was restrictive in the sense that it could only be applied to homogeneous atmospheres with the same optical properties. Wiscombe (1977) expanded the delta-Eddington method to inhomogeneous layers by adopting the parameterized values of Joseph and then solving the resulting differential equations by a matrix method solution. This was possible because he made the assumption that flux continuity is enforced at the layer interfaces. Wiscombe's methodology yielded very accurate diffuse solar fluxes for inhomogeneous turbid atmospheres for a broad range of optical depths. This condition would have to be met if the flux densities from an urban PBL were to be compared for single and multiple scattering since the optical properties within the PBL change rapidly at various elevations. The simplicity of Wiscombe's approach and the accurate results of the method lead naturally to its choice as the model to convert to the thermal domain.

3.0 BASIC THEORY AND DATA BASE

Radiative transfer theory for aerosol scattering absorption is based on the Mie theory for particles whose radius is greater than 0.03 times the wavelength of the irradiating electro-magnetic wave energy. Assuming time independence, elastic scattering (no conversion from one frequency to another in the range of observation), no internal sources (e.g., thermal emission from an embedded target, like a cloud), and sufficiently rare media that each particle is separated to the extent that no interparticle shadowing occurs, the radiative transfer equation for the diffuse radiance $I(\tau,\mu,\theta)$, as lucidly presented by Shettle and Weinman (1970), is:

$$\mu \frac{dI}{d\tau}(\tau,\mu,\phi) = -I(\tau,\mu,\phi)$$
$$+ \frac{\tilde{\omega}}{4\pi} \int_{o}^{2\pi} \int_{-1}^{+1} P(\mu,\phi;\mu',\phi')I(\tau,\mu',\phi')d\mu'd\phi' \qquad (3.1)$$
$$+ \frac{\tilde{\omega}}{4} F_{o} P(\mu,\phi;\mu_{o},\phi_{o}) e^{-\frac{\tau}{\mu_{o}}}$$

where the second term is the diffuse component i.e., multiply scattered radiance (self-illumination) and the third term represents the collimated direct solar beam duly attenuated to optical depth (τ) by extinction.

The following notations and Figure 3.1, Scattering Geometry, will expound upon the elements making up the terms of Eq.(3.1).

9

Referring to Figure 3.1:

$\mu = \cos\theta$

θ = zenith angle

ϕ = azimuth angle

Θ = angle between incident and scattered radiances

z = altitude

$k_\nu(z)$ = Extinction coefficient implicitly present in the optical depth (τ). It is a bulk property of the medium derived from Mie Theory, and it is composed of four other descriptive quantities dealing with the attenuation process.

   1.) molecular absorption (k_a)

   2.) molecular scattering (k_s)

   3.) particle absorption (σ_a)

   4.) particle scattering (σ_s)

τ_ν = optical depth given by integrating the relevant vertical extinction coefficient profiles:

$$\int_z^\infty (k_a+k_s+\sigma_a+\sigma_s)\, dz$$

$\tilde{\omega}_o$ = albedo for single scattering defined as the ratio of the amount of flux scattered to that scattered and absorbed

$$(k_s+\sigma_s) \, / \, (k_a+k_s+\sigma_a+\sigma_s).$$
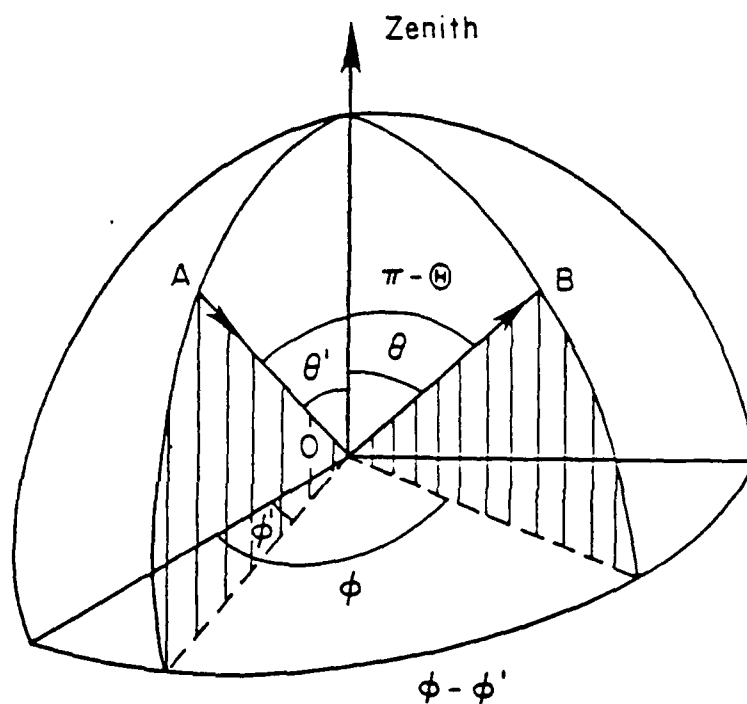
Figure 3.1 Scattering geometry showing the relationship between the zenith, azimuthal, and phase function angles (after Liou, 1980).

$P(\mu,\phi,\mu',\phi')$ = The phase function which defines the fractional amount of light incident at (μ',ϕ') which is scattered in the direction (μ,ϕ).

πF_o = Solar irradiance perpendicular to the direction of incidence.

Mie Theory provides a "complete" solution to the problem of scatter and absorption by a particle represented as an isolated isotropic sphere. The scattering properties depend on the size of the sphere, the wavelength of the incident flux, and the real and imaginary parts of the complex index of refraction. The size values are related in the Mie factor (α) defined by

$$\alpha = 2\pi r/\lambda \qquad (3.2)$$

where (λ) is the wavelength and (r) is the radius of the sphere. It is the relative size of the particle in terms of wavelength which is most important for determining the scattering process. When the particle is far smaller than the wavelength, the scattering is called Rayleigh scattering. Scattering of this type varies inversely as the fourth power of the wavelength. The principal Rayleigh scatterers in the atmosphere are the molecules of the constituent gases ($\alpha < 0.03$).

Cloud and aerosol particles are a different matter. Atmospheric particles fall broadly into four categories. (1) Solid aerosols of mean size between 0.1 and 1 μm; they are not necessarily spherical and their refractive index may be highly vari-

able. (2) Haze water drops of mean size between 0.1 and 1μm; they are spherical and have known composite refractive indices. (3) Cloud water drops of mean size between 1 and 100 μm; again spherical and of a known refractive index. (4) Cloud ice particles of mean size between 1 and 100 μm; irregular shape but known refractive index. Therefore, the relative size factor (α) becomes even more important since the scattering pattern in three dimensions changes dramatically as the radius of the particle increases along with changes in the absorption qualities of the aerosol particle in question.

3.1 Single vs Multiple Scattering

Single scattering assumes that the particle is exposed only to the light of an incident beam. No account is taken of the fact that each particle in a scattering volume is exposed to and also scatters a small amount of radiation already scattered by other particles. The LOWTRAN models prior to the release of LOWTRAN 7 only included the effects of single scattering and then only as a loss mechanism whereby scattering was not considered as a source mechanism for the path radiance. Therefore, single scattering only depleted the number of photons from a scattering volume not allowing the input from more distant sources.

Multiple scattering, on the the other hand, includes higher orders of scattering when each particle is exposed to, and also scatters light which has already been scattered by

other particles. Obviously, multiple scattering is an important process for the transfer of radiant energy in the atmosphere, particularly, when aerosols are involved. Multiple scattering allows the possibility of a global intervention from particles in the far field. This multiplicity enhances the probability that a given photon will be absorbed and/or scattered. This is so because the effective path length is increased in the presence of radiatively active gases and aerosols.

3.1.1 Absorption-Emission

Scattering is often accompanied by absorption. Both processes remove flux from a given beam of light. Scattering is explained in terms of the wave theory of light and it produces no net change in the internal energy states of the molecules. Absorption, however, requires quantum theory for its explanation and does produce changes in energy states. Three forms of internal energy exist: (a) rotational, (b) vibrational, and (c) electronic states. The incident radiation is regarded as being quantized and as such only whole quanta can be accepted by the absorbing molecule. In absorbing a quantum of energy the molecule undergoes a transition from a lower to a higher state of one of the three internal energy forms. When absorption is significant for a particular aerosol, this fact is expressed in the imaginary portion of the complex index of refraction. The larger this number is the greater the amount of energy which can be taken out by absorption.

Absorption is only the first part of a cycle which is completed by emission. As a consequence of molecular motions and collisions, molecules endlessly exchange internal for translational energy, and vice versa. Molecules already excited to upper levels are "relaxed", while molecules at lower levels are "excited" to upper levels by collisions with both events operating on a statistical basis. Most of the upper levels are inherently unstable, however, and molecules occupying these levels undergo a transition to lower levels by emitting quanta of radiant energy. The above physical activities form the basis behind blackbody radiation theory. Emission is as spectrally selective as absorption and is a discontinuous process. The difference between the flux removed from an incident beam and the totally scattered flux must be attributed to absorption by the particle. The absorbed energy goes into heating the particles which as described above leads to further emission. A cycle in which the medium surrounding the particles is heated leading to changes in the ambient environment due to the presence of aerosols.

3.2 Bulk Properties From Mie Theory

In the field of light scattering and radiative transfer, it is customary to use a term called cross-section, which is analogous to geometrical area, to denote the amount of energy removed from the beam by particles. In the case when the cross-section refers to a particle, its units are in area (cm^2)

as given in cgs units. Thus, the extinction cross-section, in units of area, is the sum of the scattering and absorption cross-sections. However, when the cross-section is in reference to a unit mass, its units are in area per mass $(cm^2 g^{-1})$. The mass extinction cross section is therefore the sum of the mass absorption and mass scattering cross-sections. Furthermore, when the extinction cross-section is multiplied by the particle number density (cm^{-3}) or when the mass extinction cross-section is multiplied by the density (gcm^{-3}) the quantity is referred to as extinction coefficient, which has units of length either (cm^{-1}) or as with LOWTRAN (km^{-1}). In the field of infrared radiative transfer the mass absorption cross-section is simply referred to the absorption coefficient as cited by Liou (1980).

Since the particles occupying a particular volume normally have a size distribution (such that the total number of particles $n_t = \int_0^\infty n(r)\, dr$ where $n(r)$ is the number of particles with radii from (r) to $(r+1)$, the mass or (volume) extinction coefficients and the phase function of a unit volume of the medium must be calculated from appropriate integrals over all the particles. That is:

$$\beta_{sc} = \int_0^\infty J(r)\, n(r)\, dr \qquad (3.3)$$

$$\beta_e = \int_0^\infty K(r)\, n(r)\, dr \qquad (3.4)$$

$$P(\theta) = 1/\beta \int_0^\infty n(r)\, J(r)\, P(r,\theta)\, dr \qquad (3.5)$$

where $J(r)$, $K(r)$ and $P(r,\theta)$ are the scattering and extinction

coefficients and the phase functions appropriate to the indivi-
dual particles of radius (r) (Paltridge and Platt, 1976).

3.2.1 Efficiency Factors and Refractive Index

The single particle scattering and extinction coefficients
$J(r)$ and $K(r)$ are normally given in terms of an expression for
the corresponding efficiency factors Q_{sc} and Q_e which are sim-
ply the ratios of $J(r)$ and $K(r)$ to the geometric cross section
πr^2. Thus according to Paltridge and Platt (1976):

$$Q_{sc} = J(r)/\pi r^2 = 2/\alpha^2 \sum_{n=1}^{\infty} (2n+1) (a_n a_n^* + b_n b_n^*) \qquad (3.6)$$

and

$$Q_e = K(r)/\pi r^2 = 2/\alpha^2 \sum_{n=1}^{\infty} (2n+1) \text{ Real } (a_n + b_n) \qquad (3.7)$$

where the a_n and b_n are complex quantities, taken from Mie
theory, which depend on the size parameter (α) and the complex
index of refraction (m).

When absorption occurs the index of refraction becomes

$$m = m_r - im_i \qquad (3.8)$$

with m_r and m_i representing the real and imaginary parts of the
complex index of refraction, and (i) the imaginary unit. The
imaginary portion carries the value of the amount of absorption
taking place when electro-magnetic radiation interacts with a
material substance. These are usually laboratory measurements
under controlled conditions. Figure 3.2 shows the scattering
efficiency factor Q_{sc} as a function of the size parameter (α)
for $m_r = 1.33$ with several differing values of the imaginary
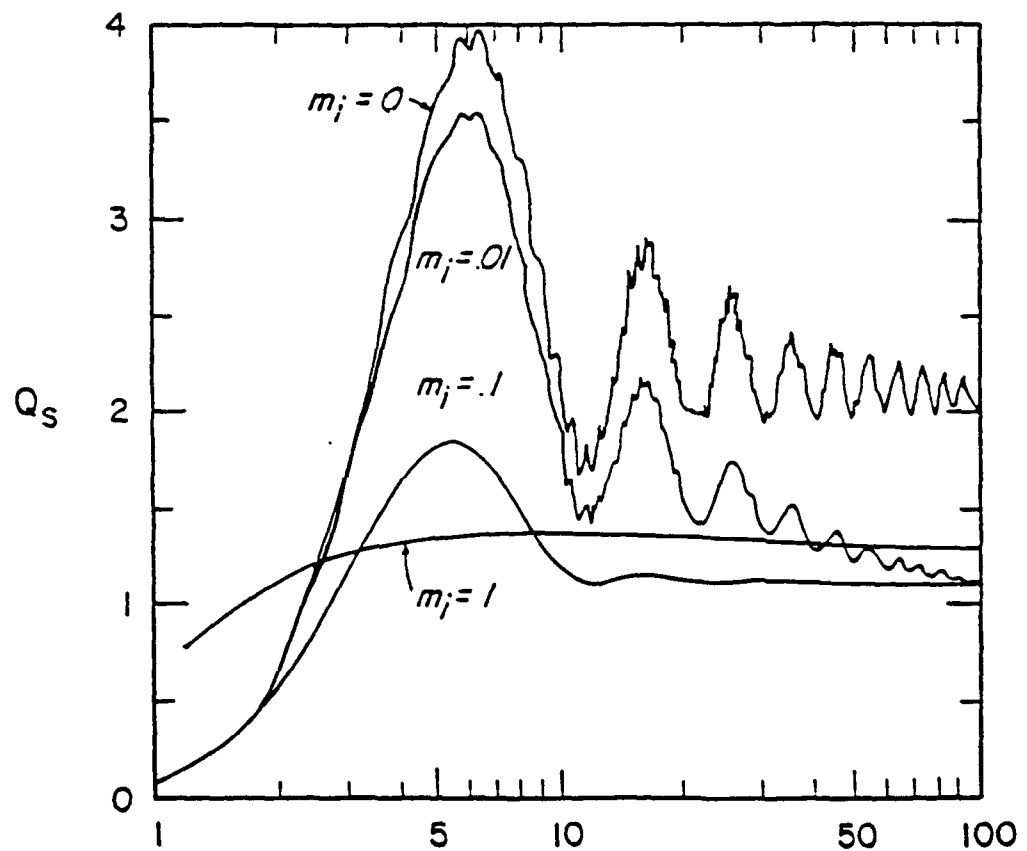
Figure 3.2 Efficiency factor for scattering, Q_s, as a function of the size parameter $\alpha = 2\pi r/\lambda$. The refractive index in $m_r = 1.33$, with results shown for four values of m_i (after Hansen and Travis, 1974).

portion. For $m_i = 0$,and the condition of a perfect reflector, there is no absorption, so that $Q_{sc} = Q_e$. Q_{sc} in this case shows a series of major maxima and minima with ripples. The major maxima and minima are due to the interference of light refracted and transmitted by the sphere, whereas the ripples arise from edge rays that are grazing and traveling along the sphere, spewing off energy in all directions. Q_{sc} or Q_e increases rapidly when the size parameter reaches about five and approaches an asymptotic value of two there after. This implies that a large particle removes from the incident beam exactly twice the amount of light that it can intercept geometrically. Physically, the removal of the incident light beam includes the diffracted component, which passes by the particle, plus the light scattered by reflection and refraction within the particle. Both the *ripples* and the *major maxima* and *minima* damp out as absorption within the particle increases.

3.2.2 Phase Function and Single Scattering Albedo

The phase function for scattering expresses in a formal manner the angular dependence of scattering on the "viewing" angle. It is defined by van de Hulst (1957) "as the ratio of the energy scattered per unit solid angle in this (a given) direction to the average energy scattered per unit solid angle in all directions." This is symbolically represented either by

$$P(\theta) = P(\mu,\phi;\mu',\phi') \qquad (3.9)$$

where as stated earlier the θ is the angle between the incident

and scattered fluxes (scattering angle).

Related to the phase function is the asymmetry factor (g or $\langle\cos\theta\rangle$). This quantity physically represents the difference between the flux densities in the forward direction and the backward direction arising from the scattering by a volume (or particle) when the incident flux is normalized to unity. This forward minus backward over the total scatter ratio is defined as the integral over all solid angles of the phase function. That is the first moment expression:

$$\langle\cos\theta\rangle = \int_{-1}^{+1} P(\theta)\cos(\theta)d(\cos\theta). \qquad (3.10)$$

It is the minimal information required about the phase function which allows some accuracy in the approximate solutions of a transfer problem. It is equal to zero for isotropic scattering (i.e., the same intensity over both hemispheres), and to +1 and -1 for complete scattering into the forward and backward directions, respectively.

The asymmetry parameter is particularly useful when multiple scattering effects are significant because the details of the scattering phase function tend to be smoothed out. This is when the asymmetry parameter is used to characterize the angular distribution of the radiation field since approximate methods like the Eddington and two-stream assume isotropy of the radiance in the forward and backward directions to model the azimuthally averaged phase functions pertinent to these methods.

3.3 Two-stream and Eddington Multiple Scattering Approximations

The Eddington and its close relative the delta-Eddington approximations are both members of the two-stream family of approximations for multiple scattering. My reasons for choosing the Eddington method was based on the following favorable attributes: (1) It provides some qualitative insight into the mechanisms whereby radiation is transferred within turbid atmospheres of moderate or large optical depths. (2) It allows rapid calculation of flux densities $F\uparrow, F\downarrow$ within realistic inhomogeneous atmospheres with an accuracy of several percent compared to more exact methods like the discrete-ordinate method of Liou (1973). (3) The method's simple approximation to a complex physical process allows numerification by standard matrix inversion techniques as suggested by Wiscombe (1977).

For all the two-stream approximations, three assumptions are made which help simplify the formulation of the governing equations. First, the transfer of radiation will occur in a horizontally plane-parallel atmosphere. Second, the radiation emission will be isotropic. Third, the upward and downward radiances, I^+ and I^-, at each level are replaced by the hemispherically integrated average radiance given by the zeroth order expression

$$\overline{I}^{\pm} = \int_{0}^{\pm 1} I \, \mu_o d\mu. \tag{3.11}$$

This allows a complex scattering pattern to be represented by

an average intensity and when integrated over azimuth an isotropic quality. Taken together they allow a method whereby the radiation field can be specified in terms of only the upward and downward components of the flux density, $F\uparrow$ and $F\downarrow$, respectively. The irradiances are then directly related to the radiance by:

$$F\uparrow = \pi \ I^{+}$$
$$F\downarrow = \pi \ I^{-}. \tag{3.12}$$

The Eddington approach assumes that the radiances can be given by a Taylor's series expansion, vis.

$$I(\tau,\mu) = I_{o}(\tau) + I_{1}(\tau)\mu \tag{3.13}$$

where all higher order terms are neglected. Figure 3.3 shows visually a comparison between the two methods together with their respective expressions for the flux densities. Each method contains its own phase function in terms of the asymmetry factor $\langle\cos\theta\rangle$. Thus for the two-stream case (Fig 3.3b)

$$P(\theta) = 1\pm\langle\cos\theta\rangle, \tag{3.14}$$

and for the Eddington approximation (Fig 3.3c)

$$P(\theta) = 1+3\langle\cos\theta\rangle\cos(\theta). \tag{3.15}$$

As stated by Paltridge and Platt (1976), "Despite the fact that the two-stream and Eddington approximations are limited in applications to cases where the scatter is not highly anisotropic, they are highly valuable because of the simplicity of their analytical solution. Further, they retain a measure of directness in physical conception which allows easy and unambiguous formulation of the boundary conditions in specific

Two stream

$F\uparrow = \pi I\uparrow$ $\qquad$ $F\uparrow = \pi I^{+}$ $\qquad$ $I = I_0 + I_1 \cos\theta$

$F\downarrow = \pi I\downarrow$ $\qquad$ $F\downarrow = \pi I^{-}$ $\qquad$ $F = \pi (I_0 \pm \frac{2}{3} I_1)$

Eddington

(a) $\qquad\qquad$ (b) $\qquad\qquad$ (c)
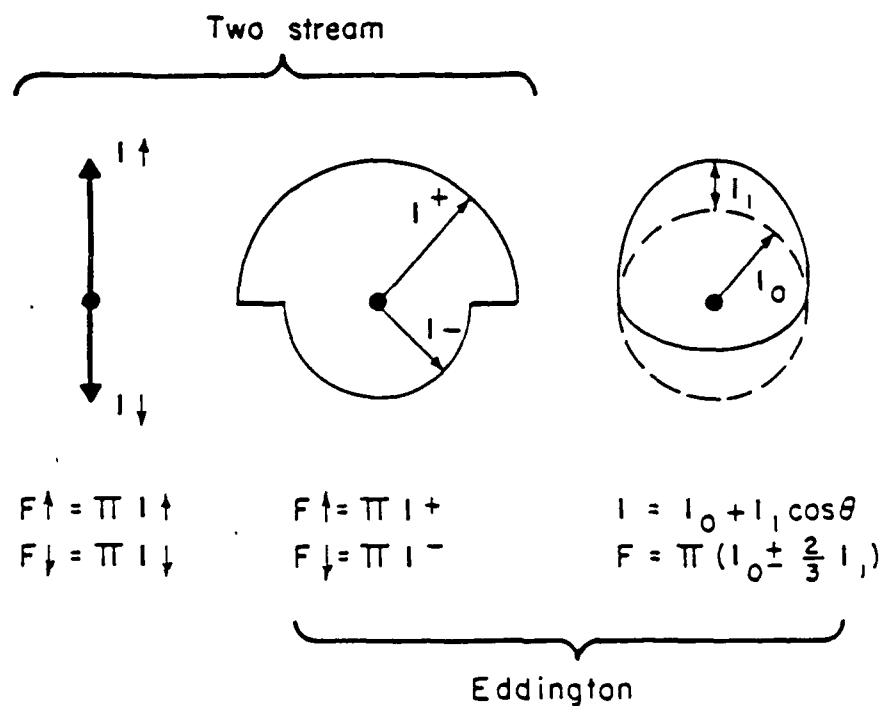
Figure 3.3 Two-stream and Eddington approximations. (a) equivalent, (b) and (c) are conceptually equivalent (after Paltridge and Platt, 1976).

23

cases."

3.4 Pertinent Data Base

The primary optical values needed to develop a multiple scattering two-stream model with a minimum of inaccuracy are the optical depths (τ), single scattering albedos (ω), and the asymmetry factors (g) for each relevant layer. As defined above these values explicitly depend upon the efficiency factors outlined previously. Few aspects of scattering have greater importance or have attracted greater attention than atmospheric scattering and extinction and the associated matter of visibility. Table 3.1 gives a listing of some of the published efficiency factors applicable to atmospheric particles. Similar sources exist for molecular scattering. Specifically, Elterman (1968,1970) tabulated values of the volume coefficients for many altitudes from sea-level to 50 km. My primary source for the optical properties came from a compilation by Shettle and Fenn (1979) which centered on lower atmospheric aerosol models. The aerosol properties were based upon experimental measurements that were made during and prior to the mid-1960's. The optical properties of the models are given for a number of wavelengths between 0.2 and 40.0 μm and for different relative humidities ranging from o to 99%. Specific to my topical objective, the investigation of multiple versus single aerosol scattering in the terrestrial infrared domain, I chose a summertime mid-latitude urban model for investigation.

Reference	Refractive index*	Size parameter
Holl (1948)	1.33	4.8, 5.4, 6.0, 6.6 (24 values) 8.0
Lowan (1949)	1.33, 1.44, 1.55, 2.00, 1.50	0.5 (15 values) 6.0 0.5 (24 values) 12.0
Houghton and Chalker (1949)	1.33	7 (33 values) 24
Gumprecht and Sliepcevich (1951b)	1.2, 1.33, 1.4, 1.44, 1.5, 1.6	1 (many values) 8, 10(5)100(10)200 (50)400
Johnson et al. (1954)	Complex values, $3.6 < \lambda < 13.5 \, \mu m$	1 (many values) 25
Pangonis et al. (1957)	1.05(0.05)1.30	0.2(0.2)7.0(1)15
Havard (1960)	Complex values, $3.6 < \lambda < 13.5 \, \mu m$	For particle $r =$ 1, 2, 4, 9, 12, 15 μm
Deirmendjian (1963b)	Complex values, $8.15 < \lambda < 16.6 \, \mu m$	0.5(0.5)7.0, 10.0, 15.0
Penndorf (1956, 1957c)	1.33; 1.40, 1.44, 1.486, 1.50	0.1(0.1)30.0
Giese et al. (1961)	1.5	0.2(0.2)159
McCormick (1967)	1.5	0.01(0.01)2.0(0.1) 181.9
Irvine and Pollack (1968)	Complex values, $0.7 < \lambda < 200 \, \mu m$	For particle $r =$ 0.3, 1, 3, 10 μm
Zelmanovich and Shifrin (1968)	Various complex values	0.5 (many values) 100

Table 3.1 Published tabulations of efficiency factors applicable to atmospheric particles (after McCartney, 1976).

The attenuation coefficients for the different aerosol models (urban, rural, maritime, and tropospheric) are given in a tabular form and allow extrapolation for the desired wavenumber domain. An example of such a table is presented below in Table 3-2.

TABLE 3.2: Attenuation coefficients, single scatter albedo, and asymmetry parameter for relative humidity = 80% urban model (after Shettle and Fenn, 1979).

| WAVELENGTH (MICRON) | NORMALIZED TO A NUMBER DENSITY OF 2.0000E+04 PARTICLES/CM3 | | | | |
	EXTINCTION (KM-1)	SCATTERING (KM-1)	ABSORPTION (KM-1)	SINGLE SCAT.ALB.	ASYMMETRY PARAMETER
.200	7.075E-01	5.099E-01	1.976E-01	.7208	.7949
.300	5.908E-01	4.572E-01	1.336E-01	.7738	.7713
.337	5.489E-01	4.274E-01	1.215E-01	.7786	.7650
.550	3.602E-01	2.811E-01	7.906E-02	.7805	.7342
.694	2.799E-01	2.158E-01	6.407E-02	.7711	.7162
1.060	1.666E-01	1.199E-01	4.670E-02	.7197	.6873
1.536	1.033E-01	6.784E-02	3.550E-02	.6565	.6820
2.000	7.316E-02	4.505E-02	2.811E-02	.6158	.7131
2.250	6.477E-02	3.896E-02	2.581E-02	.6015	.7312
2.500	5.799E-02	3.353E-02	2.446E-02	.5782	.7583
2.700	5.624E-02	2.540E-02	3.083E-02	.4517	.8030
3.000	9.536E-02	2.463E-02	7.073E-02	.2587	.7171
3.392	5.566E-02	3.144E-02	2.421E-02	.5650	.7185
3.750	4.806E-02	2.971E-02	1.915E-02	.6081	.7400
4.500	4.401E-02	2.486E-02	1.915E-02	.5648	.7698
5.000	4.092E-02	2.332E-02	1.760E-02	.5699	.7778
5.500	3.781E-02	2.116E-02	1.665E-02	.5597	.7923
6.000	4.219E-02	1.492E-02	2.727E-02	.3536	.8142
6.200	4.233E-02	1.748E-02	2.484E-02	.4131	.7864
6.500	3.744E-02	1.838E-02	1.907E-02	.4908	.7867
7.200	3.517E-02	1.679E-02	1.838E-02	.4775	.7891
7.900	3.040E-02	1.336E-02	1.704E-02	.4394	.8147
8.200	2.901E-02	1.091E-02	1.810E-02	.3760	.8298
8.700	3.941E-02	1.719E-02	2.222E-02	.4362	.7276
9.000	4.085E-02	1.718E-02	2.367E-02	.4205	.7136
9.200	3.985E-02	1.517E-02	2.468E-02	.3806	.7361
10.000	3.134E-02	1.372E-02	1.762E-02	.4379	.7590
10.591	2.890E-02	1.163E-02	1.727E-02	.4024	.7729

4.0 PROCEDURAL RESEARCH METHODOLOGIES

4.1 Overview

The topical objective of comparing aerosol single scattering versus multiple scattering in the terrestrial long wavelength domain requires the development of a suitable algorithmic procedure to calculate the desired fluxes. Shettle and Weinman (1970) developed an Eddington formulation which dealt exclusively with solar fluxes. Their method was extended to the infrared regime by manipulation of the basic radiative transfer equation. A computer code analogous manner to Wiscombe's (1977) was constructed based on the delta- Eddington approximation of Joseph et al. (1976).

This numerical model produces flux densities. However, validation procedures and comparative verification indicate that my development is not suitable. In search for a modified approximation, I turned to the recently released LOWTRAN 7 which does contain a multiple scattering routine for the longwave domain. The insight gained from the first endevour, allows me to see the superiority of the LOWTRAN 7 two-stream and adding method. It is to be my primary tool into the investigation of the scientific problem.

4.2 Derivation of Eddington Modification

The development of a computer code suitable for determining multiply scattered thermal radiation begins with a suggestion by Liou (1980). He indicates that for the transfer of terrestrial infrared radiation in scattering atmospheres, which are in local thermodynamic equilibrium, it is possible to replace the last term in Eq. (3.1) by a term representing a thermal emission contribution, vis.,

$$(1-\tilde{\omega}_\nu)[B_\nu(T(\tau))] \tag{4.1}$$

where $\tilde{\omega}_\nu$ is the single scattering albedo and B_ν is the Planck function of temperature (T). The subscript ν, dropped later, signifies that a spectral density function is explicitly understood. The temperature (T) is also dependent upon the optical depth (τ) which in this development is taken to be the vertical coordinate for the used reference system. Using Eq. (4.1) in Eq. (3.1) yields:

$$\mu \frac{dI}{d\tau}(\tau,\mu,\phi) = -I(\tau,\mu,\phi)$$

$$+ \frac{\tilde{\omega}}{4\pi} \int_0^{2\pi} \int_{-1}^{+1} P(\mu,\phi;\mu',\phi')I(\tau,\mu',\phi')d\mu'd\phi' \tag{4.2}$$

$$+ (1-\tilde{\omega}_\nu)[B_\nu(T(\tau))]$$

where the wavenumber dependence is understood. Term one on the right, $I(\tau,\mu,\phi)$, is the spectral radiance of the diffuse radiation field. Term two represents the multiply scattered diffuse component, and term three is the thermal emission contribution

from optical depth τ. Eq. (4.2) becomes the starting point for a procedure outlined by Shettle and Weinman (1970) to construct an Eddington approximation leading to two ordinary differential equations which when solved analytically produce simple exponential solutions for the flux densities.

Eddington's approximation assumes the radiance can be given by

$$I(\tau,\mu) = I_0(\tau) + \mu I_1. \qquad (4.3)$$

If the phase function is expanded as a series of associated Legendre functions, in the manner of Chandrasekhar (1960), and that Eq. (4.3) represents the diffuse radiance, all terms of orders greater than one will vanish when Eq. (4.1) is integrated over (μ) and (ϕ). The phase function then may be approximated by

$$P(\cos(\Theta)) = 1+\omega_1(\tau) \cos(\Theta) \qquad (4.4)$$

where Θ is the angle between the incident and scattered radiances (scattering angle). The integral in Eq. (4.1) then becomes

$$\int_0^{2\pi} \int_{-1}^{1} P(\mu,\phi;\mu',\phi')I(\mu',\phi')d\mu'd\phi' = 4\pi(I_0+\mu g I_1) \qquad (4.5)$$

where

$$g = \frac{\tilde{\omega}_1}{3} = 1/2 \int_{-1}^{+1} P(\Theta) \cos\Theta \, d\cos(\Theta). \qquad (4.6)$$

is the asymmetry factor. Using Eq. (4.6) in Eq. (4.1) after integrating over ϕ and dividing by 2π produces

$$\mu \left(\frac{dI_o + \mu I_1}{d\tau}\right) = -(I_o + \mu I_1)$$
$$+ (1 - \tilde{\omega}_v)[B_v(T(\tau))]. \qquad (4.7)$$

A differential equation is obtained for I_1 by integrating Eq. (4.7) over μ from -1 to $+1$ leading to:

$$\frac{dI_1}{d\tau} = 3(1 - \tilde{\omega})(B(T(\tau)) - I_o). \qquad (4.8)$$

$\frac{dI_o}{d\tau}$ is produced by multiplying Eq. (4.7) by (μ) then integrating over μ from -1 to $+1$ to generate:

$$\frac{dI_o}{d\tau} = -I_1(1 - \tilde{\omega}g). \qquad (4.9)$$

These two simultaneous differential equations can be solved by substitution and standard techniques. Starting with Eq. (4.9) and taking the derivative of both sides along with a substitution from Eq. (4.8) leads to:

$$d^2I_o / d\tau^2 = -3(1 - \tilde{\omega})(1 - \tilde{\omega}g) (B(T(\tau)) - I_o). \qquad (4.10)$$

Letting $K_o = 3(1 - \tilde{\omega})(1 - \tilde{\omega}g)$ and rearranging produces a differential equation in standard form;

$$d^2I_o/d\tau^2 - K_o I_o = -K_o B(T(\tau)). \qquad (4.11)$$

To solve this equation a general solution is needed composed of a complementary and particular solution vis.,

$$I_{oc} = A_i \exp(\sqrt{k_o}\tau) + B_i \exp(-\sqrt{k_o}\tau). \qquad (4.12)$$

The particular solution will include a Planck function which in its unabridged wavenumber form is given by Walker (1960) as

$$B_v(T) = c_1 v^3 (\exp(-c_2 v/T) - 1). \qquad (4.13)$$

Here c_1 is $(2hc^2)$ where (h) is Planck's constant and (c) is the

speed of light in the vacuum. This term in cgs units equals 1.1909×10^{-12} watts $cm^2 sr^{-1}$. C_2 is made up of Planck's constant, the speed of light and Boltzmann's constant combined algebraically into (hc/k) to yield in cgs units 1.438 cm $K°$. However, numerically, this form proves to be cumbersome in the derivation of the differential equations. I decided to follow Wallace and Hobbs (1976) and use a truncated Planck expression given by:

$$B_\nu(T(\tau)) = c_1 \nu^3 \exp(-c_2 \nu/T). \qquad (4.14)$$

This is done because throughout most of the wavenumber domain the exponential term in the untruncated version is normally much larger than unity. Only at the smaller wavenumbers (≥ 850 cm^{-1}) does the full expression become necessary. Testing indicates that a 4.0% error is incurred over the temperature range used in the models. Therefore, Eq. (4.11) becomes

$$d^2 I_o/d\tau^2 - K_o I_o = -K_o c_1 \nu^3 (\exp(-c_2 \nu/T(\tau))). \qquad (4.15)$$

The RHS of Eq. (4.15) is of the form $(K e^{cx})$ where (K) and (c) are constants and (τ) is the independent variable. This implies that the particular solution is simply some multiple of $e^{c\tau}$. Assuming that the particular solution I_{op} is equal to

$$F e^{-c_2 \nu/T(\tau)} = I_o \qquad (4.16)$$

and

$$K_1 = -K_o c_1 \nu^3 \qquad (4.17)$$

with substitution into Eq. (4.15) yields

$$K_1 e^{-c_2 \nu/T(\tau)} = (F e^{-c_2 \nu/T(\tau)})'' - K_o F e^{-c_2 \nu/T(\tau)}. \qquad (4.18)$$

Implementing the 2nd derivative and solving for F along with substitution for K_1 produces

$$F = \frac{K_0 c_1 \nu^3 T^3}{2c_2(\Delta T/\Delta \tau)^2} - \frac{K_0 c_1 \nu T^4}{c_2(\Delta T/\Delta \tau)^2} + c_1 \nu^3 \qquad (4.19)$$

which has units of radiance, watts cm^{-2}, when multiplied by $e^{-c_2\nu/T}$.

The $\Delta T/\Delta \tau$ elements in Eq. (4.19) represent the differential $dT/d\tau$ which is implicit in the derivative of Eq. (4.18). No explicit relationship can be easily obtained for $dT/d\tau$ because of the non-linear dependency of the extinction coefficient on the number density, gas pressure, and temperature. Therefore, a linear approximation is made with the input parameters ΔT and $\Delta \tau$ determined from the LOWTRAN output. The change in temperature (ΔT will come from arbitrary established levels and the changes in optical depth $\Delta \tau$ will come from the wavenumber dependent mean transmittances (Tr) given by:

$$\Delta \tau = -\ln(Tr). \qquad (4.20)$$

The general solution for Eq. (4.15) is

$$I_0 = A_1 e^{\sqrt{k_0}\tau} + B_1 e^{-\sqrt{k_0}\tau} + F e^{-c_2\nu/T} \qquad (4.21)$$

where A_1 and B_1 are unknown arbitrary constants.

Similarly, a solution for I_1 yields

$$I_1 = A e^{\sqrt{k_o} \tau}$$
$$+ B e^{-\sqrt{k_o} \tau} \tag{4.22}$$
$$+ D e^{-c_2 v/T}$$

where

$$D = \frac{3(1-\omega)(1-\omega g)c_1 v^3 T}{2c_2(\Delta T/\Delta \tau)}$$
$$+ \frac{3(1-\omega)(1-\omega g)c_1 v^2 T^2}{c_2(\Delta T/\Delta \tau)} \tag{4.23}$$
$$+ \frac{c_1 c_2 v^4 T^{-2}}{(1-\omega g)(\Delta T/\Delta \tau)}$$

which also has units of radiance when multiplied by $e^{-c_2 v/T}$.

4.2.1 Computer Code Adaptation of Eddington Approximation

Joseph, Weinman, and Wiscombe (1976) discovered the excellent accuracy of the delta-Eddington approximation for solar radiative flux (which calculates flux directly) for all phase functions, no matter how asymmetric, and for all optical depths and single scattering albedos. However, that work only investigates homogeneous layers. Wiscombe (1977) developed an inhomogeneous multi-layer version. I followed Wiscombe's procedure to develop a code which could generate fluxes for the thermal domain based upon the Eddington approximation of Shettle and Weinman (1970). The solution for solar flux in the delta-

Eddington method is equivalent to the Eddington approximation without the transformed parameters g', ω', and τ' of Joesph et al (1976). Thus, I feel justified in attempting to expand Wiscombe's numerical procedure to longer wavelengths.

Accordingly, the diffuse irradiances may be computed from I_o and I_1 from

$$F^{\pm} = \pi \ [I_o(\tau) \pm 2/3 \ I_1(\tau)], \qquad (4.24)$$

or in Wiscombe's notation

$$G = \pi \ I_o, \quad H = 2/3 \ \pi \ I_1 \qquad (4.25)$$

from which

$$F\uparrow = \pi(I_o - 2/3 \ I_1) = G - H$$
$$\qquad (4.26)$$
$$F\downarrow = \pi(I_o + 2/3 \ I_1) = G + H$$

If the atmosphere is subdivided in such a way that the optical properties: optical depth, single scattering albedo, and asymmetry factor all are constant within any layer then the complete layer structure can be modeled as a concatenation of N-1 homogeneous sublayers as depicted in Figure 4.1. Here level (i+1) is topped by layer (i) with the vertical coordinate being the optical depth whose value is 0 at $\tau(0)$ and $\tau^*(N)$ at level N. By imposing top and bottom boundary conditions and requiring flux continuity across interior levels (interfaces) a system of simultaneous differential equations can be developed represented at layer (i) as
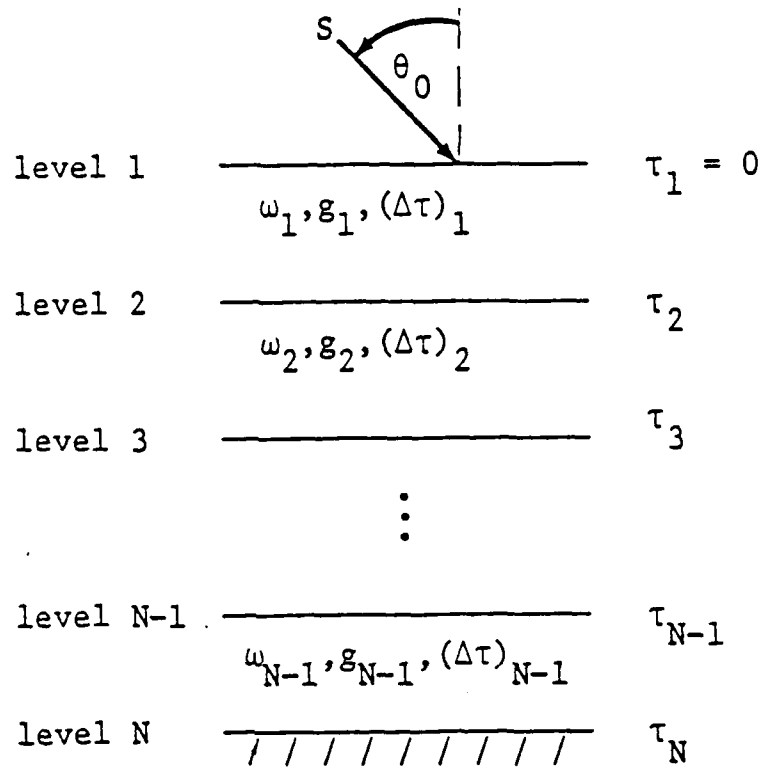
Figure 4.1 Schematic presentation of Eddington modification atmosphere which is a concatenation of N homogeneous layers with layer values of single scattering albedo (ω_i), asymmetry factor (g_i) and layer optical depth $\Delta\tau_i$). τ_{N-1} is the total optical depth at level N with S being the incident solar flux at N=1.

$$G_i = \pi \, [x_{2i-1} \exp(\lambda_i \tau_i)$$
$$+ x_{2i} \exp(-\lambda_i \tau_i) \qquad (4.27)$$
$$+ \alpha_i \exp(-c_2 \nu/T)]$$

and

$$H_i = -2/3\pi \, [x_{2i-1} \exp(\lambda_i \tau_i)$$
$$+ x_{2i} \exp(-\lambda_i \tau_i) \qquad (4.28)$$
$$+\beta_i \exp(-c_2 \nu/T)]$$

where α_i and β_i are from Eqs. (4.19 and 4.23) and λ_i is $\sqrt{k_o}$ from Eq.(4.10). The unknown constants for layer i are written in the notation

$$x_{2i-1} = A_i, \qquad x_{2i} = B_i$$

in order that the usual matrix/vector notation (C $\hat{x}$ = D) for a linear system of equations might subsequently be applied. The construction of the matrix system of equations rests upon the assumption of flux continuity at the interface between layers and solving for the unknown constants. Appropriately, the inte-rior flux continuity conditions are represented by

$$G_{n-2}(\tau_{n-1}) - G_{n-1}(\tau_{n-1}) = 0$$
$$\qquad (4.29)$$
$$H_{n-2}(\tau_{n-1}) - H_{n-1}(\tau_{n-1}) = 0$$

which form a couple for each layer, where $\tau_2 \ldots \tau_{n-1}$ are the level values of optical depth from the top to level N. Each set must be solved to find the unknown constants x_{2i-1} and x_{2i}. The flux continuity conditions Eqs. (4.29) are expressed in terms of G and H rather than the flux density terms (F↑= G-H) and (F↓=G+H). This is because, by doing so, the coefficients have a simpler form, and numerically ill-conditioning is avoided.

Attempts to solve Eqs. (4.29) directly would lead to insurmountable ill-conditioning for the layers, no matter how they were subdivided. This is directly traceable to the exponentials $e^{(\lambda_i \tau_i)}$ and $e^{(-\lambda_i \tau_i)}$ in Eqs. (4.27 and 4.28) which become very large and very small for increasing optical depths (τ_i), respectively. Wiscombe observed that the flux density formulas at each level required, not the bare quantities x_i but rather

$$\hat{x}_{2i-1} = e^{\lambda_i \tau_{i+1}} x_{2i-1}$$
$$\hat{x}_{2i} = e^{-\lambda_i \tau_{i+1}} x_{2i}$$

(4.30)

which come about because of the requirement for flux continuity across the interfaces. Substitution of Eqs. (4.30) into (4.27) and (4.28) produce the following interior flux continuity equations:

$$\hat{x}_{2i-1} + \hat{x}_{2i} - \frac{\hat{x}_{2i+1}}{\exp(\lambda_{i+1}\Delta\tau_{i+1})} - \hat{x}_{2i+2}\exp(\lambda_{i+1}\Delta\tau_{i+1})$$

$$= \alpha_{i+1} \exp(-c_2\nu/T_{i+1}) - \alpha_i \exp(-c_2\nu/T_i)$$

(4.31)

and

$$\hat{x}_{2i-1} + \hat{x}_{2i} - \frac{\hat{x}_{2i+1}}{\exp(\lambda_{i+1}\Delta\tau_{i+1})} - \hat{x}_{2i+2}\exp(\lambda_{i+1}\Delta\tau_{i+1})$$

$$= \beta_{i+1} \exp(-c_2\nu/T_{i+1}) - \beta_i \exp(-c_2\nu/T_i).$$

(4.32)

However, this substitution will prove to be fatally flawed since then the optical properties to be considered would only

come from the layer immediately adjacent to the level under consideration. Thus not allowing the other layers to leave their "imprint" on the layers under scrutiny and not attenuating the transmitted emission. Eqs. (4.31) and (4.32), and as yet unspecified boundary conditions form the coefficient matrix C to solve for the unknown constants $\hat{x}_{2i-1}$ and $\hat{x}_{2i}$ in C $\hat{x}$ = D where D represent the constant vectors of the RHS's of Eqs. (4.31) and (4.32). The requisite interior flux formulaes at each level (i+1) would be:

$$F^\uparrow_{i+1} = 5/3\pi[\hat{x}_{2i-1} + \hat{x}_{2i} + (\beta_i + \alpha_i)\ \exp(-c_2\nu/T_i)] \tag{4.33}$$

and

$$F^\downarrow_{i+1} = 1/3\pi[\hat{x}_{2i-1} + \hat{x}_{2i} + (\alpha_i - \beta_i)\ \exp(-c_2\nu/T_i)]. \tag{4.34}$$

4.2.2 The Boundary Conditions

The top boundary condition poised a unique problem since the assumption of local thermodynamic equilibrium (LTE) was made. LTE does not occur within the atmosphere till approximately 45 kilometers based on considerations presented by Goody (1964). Therefore, the emissions from the layers above have to be adjusted so as not to project the full Planckian emittance. Choosing as does LOWTRAN the top of the atmosphere at 100 kilometers the Planckian function had to be scaled to perform a smooth transition to levels where LTE sets in. A

proportionality constant will be multiplied by the Planckian emission from that level reducing the output. For example, at 100 km, the constant would be As a boundary condition input, the summation of the levels would constitute a "direct" thermal (F_o) input from layers which although not at LTE, still produce an emission due to the presence of a tenuous atmosphere. The top boundary condition becomes

$$5/3\pi \frac{\hat{x}_{2i-1}}{\exp(\lambda_i\tau_2)} \cdot ce + \hat{x}_{2i}\exp(\lambda_i\tau_2)$$

$$= F_o - \exp(-c_2\nu/T_1)(\alpha_1+\beta_1). \tag{4.35}$$

The bottom boundary condition uses the common assumption of a Lambertian reflectance, i.e., the upward isotropic flux given by a constant surface albedo (A) multiplied by the downward flux, plus the emission from the underlying surface represented by:

$$c_i\nu^3 \exp(-c_2\nu/T_s)$$

produces the upward flux density from the surface. But, for a complete description, the layers approximately 1.0 km above the surface boundary are also included as suggested by Pallmann (1988) based on tables found in Goody (1964). This is accomplished by multipling the emittance from each layer within this range and duly attenuating the cumulative radiance by the optical depth of each layer. This action then represents diffuse counter-radiation which can be significant in aerosol-laden environments. The formulation then leads to an analogous expression for the bottom boundary condition used by Wiscombe for the solar regime to include the reflected radiation

(reflux), vis.,

$$\hat{x}_{2n-3}[(1-A)\pi-(1+A)2/3\pi)]$$

$$+ \hat{x}_{2n-2}[(1-A)\pi-(1+A)2/3\pi]$$

$$= \varepsilon\, c_1 \nu^3\, \exp(-c_2\nu/T_s)$$

$$+ \text{reflux}\,(1-\varepsilon).$$

(4.36)

4.2.3   Validation and Verification of the Eddington Thermal Modification

Upon activating the algorithm and programming actual runs of Eqs. (4.31) and (4.32) as submitted to the original penta-diagonal L-U decomposition matrix inversion method prove to be ill-conditioned for the generation of a non-singular result. To solve this problem I adopted a standard singular value decomposition method from Press et al. (1986), specifically designed for systems which approach the condition of singularity. Ill-conditioning of the system is avoided but the values for the fluxes are unacceptably too large when compared to the LOWTRAN 6 single scattering routine and the direct thermal emission based on the full and abridged Planck funtion. Both methods indicate that my results were anywhere from four to five orders of magnitude too large.

I believe the reason for this is that my development of the Eddington differential equations failed to produce an adequate physical model of the real attenuation process taking place in optically thick environments. The adjacent layer optical thickness, transmittance, and reflectance were not present

implicitly or explicitly in my formulation. The only input to the individual level flux values came from the layer immediately below. Thus, Wiscombe's original substitution for the $\hat{x}$ values to avoid ill-conditioning in the matrix proved not to take into account the total optical depth (τ^*) at the level under scrutiny i.e., the fluxes became isolated values. The upward and downward flux values, not duly attenuated, become inflated and do not represent the mulitple scattering taking place. It is obvious that this method is not appropriate and a replacement must found. Due to time constraints, LOWTRAN 7, the latest version of the LOWTRAN family and newly released, is chosen.

4.3 LOWTRAN 7

4.3.1 Overview

Although the Eddington modification did not prove fruitful it allowed insights into the complex nature of multiply-scattered radiation fields. The approximation, suggested by Shettle and Weinmann proved insufficient to account for all the physical processes which occur in the atmosphere in the presence of a heavily aerosol laden planetary boundary layer.

LOWTRAN 7 is capable of handling the complex multiple scattering problem by using an adding method and a k-distribution function. The k-distribution function adequately

decouples the scattering of aerosols from the absorption by gases allowing a separation of the two phenomena. This step is necessary since LOWTRAN 7 is a low spectral resolution model which does not allow line by line integration of the molecular absorption bands. The adding method algebraically combines layers to include the processes of transmission and reflection to account for the flux densities emanating upward and downward from the layer interfaces.

The following outline of the mechanics of LOWTRAN 7 originated from a technical report authored by Issacs et al. (1986). Although, this report was written for adaptation of LOWTRAN 6, the same formulations were used for both models. The other papers referred to in this section are used to clarify the applicable procedures and are duly cited.

4.3.2   Stream Approximation/Multiple Scatter Source Function

In the stream approximation, the multiple scattering contribution to the source function J_o

$$J_{MS}(\tau,\mu,\phi) = \omega_o/4\Pi \int_{\Omega'} P(\Omega;\Omega')I(\tau,\Omega')d\Omega' \tag{4.37}$$

is approximated by assuming isotropic scattering radiances I^+ and I^- over upward (Ω^+) and downward (Ω^-) hemispheres, respectively.

Substitution of the azimuthally averaged radiances into Eq. (4.37) yields:

$$J_{MS}(\tau,\mu,\phi) \approx \omega_o/4\pi \; [I^+(\tau) \int_{\Omega^+} P(\Omega,\Omega^+)d\Omega^+$$

$$+ I^-(\tau) \int_{\Omega^-} P(\Omega,\Omega^-)d\Omega^-]. \qquad (4.38)$$

This approximation is the same as that used for the Eddington method based on isotropy over the appropriate hemisphere. Integrating over the angular scattering functions for the resulting azimuthally averaged backscatter fractions, $\beta(\mu,g)$ (based on a function of zenith angle cosine and the asymmetry factor), and substituting the corresponding fluxes $I\pm(\tau) = F\pm(\tau)/\pi$ results in the multiple scattering source funtion to be:

$$J_{MS}(\tau,\pm\mu,) \approx \omega_o/\pi \; [F\pm(\tau)(1-\beta) + F\pm(\tau) \; \beta]. \qquad (4.39)$$

The quantity β is the backscatter fraction for isotropically incident radiation and is based on elliptical integrals involving the zenith angle and asymmetry factor as presented graphically in Fig (4.2). This method uses a Henyey-Greenstein (H-G) phase function and in doing so introduces a small amount of error ($\leq 3\%$). Howe er, this small error is quite acceptable compared to the advantage Hansen (1969) demonstrated when he showed that H-G function can be used to replace the more realistic Mie phase function in multiple scattering calculations with no more than a few percent error.
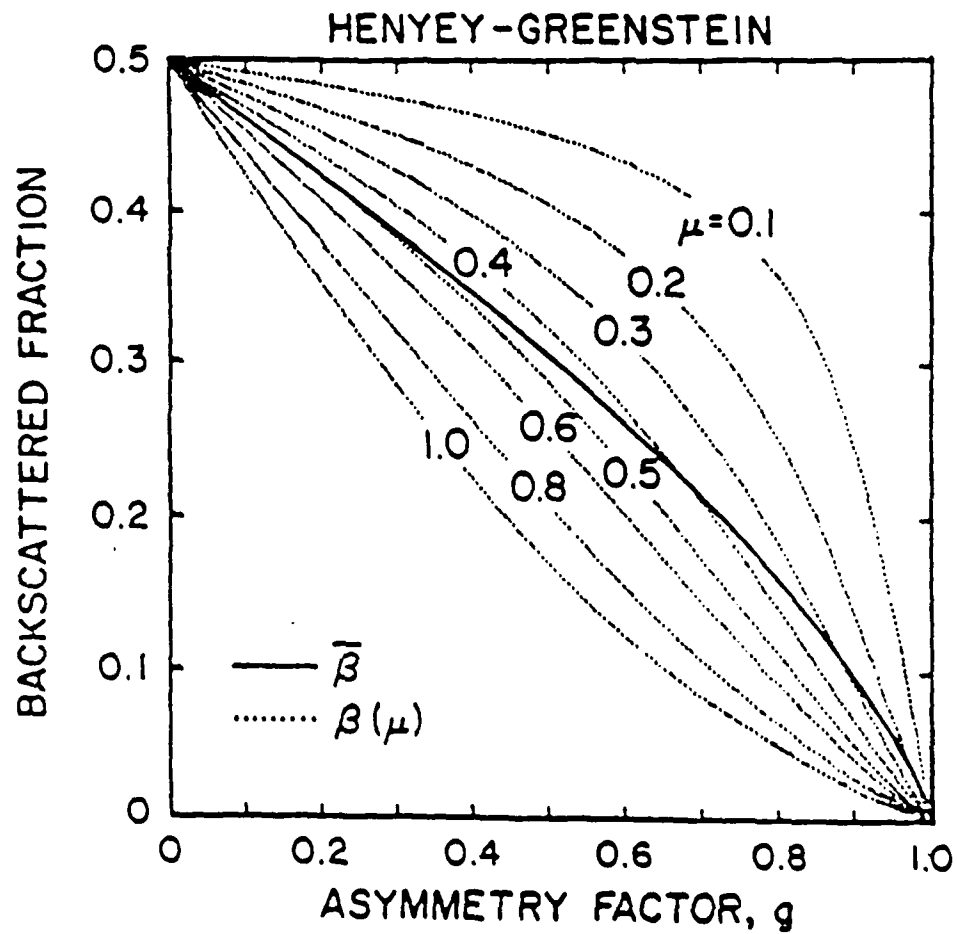
Figure 4.2 Backscattered fraction β and β(μ) for the Henyey-Greenstein phase function versus the asymmetry factor (g) for a range of values of μ (Wiscombe and Grams, 1976).

Therefore, evaluation of the approximated MS source function Eq. (4.39) requires local fluxes (F^+), and (F^-), back-scatter fractions (β), and single scattering albedos (ω_o). This expression (Eq.(4.39) is added to the thermal contribution to produce the general source function (J) given by:

$$J(\tau,\mu,) = [1-\omega_o]B[T(\tau)]$$

$$+ \omega_o/\pi \, [F\pm(\tau)(1-\beta) + F\pm(\tau) \, \beta]. \tag{4.40}$$

The source function is integrated along the desired path to obtain the desired total radiance including, now, the approximated MS contribution.

Discretizing Eq. (4.40) for a given layer, n, the contribution of multiple scattering and thermal emission is represented by:

$$j^N_{SA(\tau)} = [1-\omega_o]B(T(\tau))$$

$$+ \frac{\omega_o^N}{\pi} \, [F_N\pm(1-\beta^N)g^N$$

$$+ F_N\pm \, \beta^N g^N \,]. \tag{4.41}$$

The source function is integrated along the desired path to obtain the desired total radiance including, now, the approximated multiple scattering contribution. Here the fluxes are taken as the layer mean quantities evaluated at a level halfway through the layer. The asymmetry factor, (g), is a measure of directional scattering and is available from tabulations as in Shettle and Fenn (1970).

4.3.3   Layer Fluxes

Fluxes approximate the required radiances for evaluation of the multiply scattering source function. There are three types of fluxes. The first are the "local" fluxes ($F^{\pm}$) which are produced by each individual local layer. Next, come the "composite" fluxes ($F^{1\pm}$) which are produced by the adding method when individual intrinsic layers are combined. Finally, the "total" fluxes ($F^{2\pm}$) are generated when the adding algorithm makes its upward and downward passes through the model atmosphere layer by layer.

The local fluxes come from the flux parameterizations for each individual intrinsic layer. Included in the parameterization are the transmission (T) and reflection (R) functions based upon the formulation of the spectrally dependent flux parameterizations. The local fluxes were also calculated in the Eddington modification, however, no explicit concatenation process occurred. The approach for LOWTRAN 7 is to evaluate the local fluxes and then combine them to produce a composite flux profile using the adding method.

In LOWTRAN 7 the appropriate infrared parameterization is given by a linear Planck function relationship across an atmospheric layer. This leads to parameterizied two-stream solutions for emission from the layer top and layer bottom, and for the transmission and reflection functions given explicitly by Isaacs et al. (1986):

$$F^+ = a(PB_t - mQ - B_b) / D \qquad (4.42)$$

$$F^- = a(PB_b + mQ - B_t) / D \qquad (4.43)$$

$$T = a / D \qquad (4.44)$$

$$R = uv(e^{\tau 1} - e^{\tau 1}) / D. \qquad (4.45)$$

Here the B_t and B_b are the full Planckian function for the thermal emission at the layer top and bottom. The individual components which make up the expressions above are:

$$a = \sqrt{(1-\omega_o)} \qquad (4.46)$$

$$m = (B_b - B_t) / \tau \qquad (4.47)$$

$$P = ve^{\tau 1} + ue^{-\tau 1} \qquad (4.48)$$

$$Q = ve^{\tau 1} - ue^{-\tau 1} - a \qquad (4.49)$$

$$D = v^2 e^{\tau 1} - u^2 e^{-\tau 1} \qquad (4.50)$$

$$u = (1-a) / 2 \qquad (4.51)$$

$$v = (1+a) / 2 \qquad (4.52)$$

$$\tau 1 = \sqrt{3} \, a\tau. \qquad (4.53)$$

The optical thickness (τ) and the single scattering albedo (ω) are parameterized by the following expressions:

$$\tau = ku + \tau_s(1-g) + \tau_a \qquad (4.54)$$

$$\omega_o = \tau_s(1-g) / \tau. \qquad (4.55)$$

Here (k) is the gas absorption coefficient (for a particular

wavenumber and probability interval), (u) is the gas density, (τ_s) is the scattering optical thickness, (τ_a) is the absorption optical thickness, and (g) is the asymmetry factor for the particulate matter in the layer.

The infrared parameterization given above is significantly different from the previous derivation for the thermal fluxes, but there are some parallels. The first difference is that my method did not use the Planck function explicitly for the top and bottom emissions. But, the above method does in fact make the same assumption about a linear relationship between the Planck funtion and the change in optical depth. Another difference is that the Eddington modification did not use parameterizied values for the optical depth (thickness) or single scattering albedoes. The Eddington method used the LOWTRAN derived transmittances which inherently contain the total extinction coefficient based on molecular and particulate scattering and absorption extinction coefficients. However, the parameterization above does, like my method, use only the layer optical depths rather than the total optical thicknesses. It is justifiably done in this case because the adding method allows layer interaction explicitly while the Eddington modification did not relate the adjacent layers. Another difference is the use of the exponential terms $(e^{\pm \tau 1})$ to directly diminish or enhance the Planckian emission. My formulation relied upon the solution of the matrix vector $\hat{x}$ to solve for the fluxes at each level with the terms containing the source function used

to calculate the constant vectors. Thus, no direct scale interaction was allowed. Of course, the most significant difference lies in the fact that layer transmission and reflection functions are used to determine the intermediate composite fluxes at the layer interfaces. The modification that was attempted did not take the reflectance nor transmission value into consideration. This did not allow layer interaction which caused my flux values to become inflated. No explicit attenuation process was available to diminish the flux values.

The infrared flux parameterization then represents the complex interaction of the effects of molecular and aerosol extinction processes related to the thermal emission from an isolated layer. The ratios of single scattering albedo and asymmetry factor are used to construct a two-stream approximation for the amount of longwave radiation being generated from layer (N) based on its temperature and optical depth.

4.3.4   The Adding Method

The multiple scattering (MS) capability in LOWTRAN comes about by combining the stream approximation (SA) with the adding method to obtain the required MS flux profiles. Fundamentally, the local MS source function is composed of contributions scattered from layers, both above and below the current layer in addition to local thermal emission. Once obtained, the source function for the MS radiance may be summed along a

desired path to obtain the thermal emission via summation of the all local layer Planck function contributions.

In the adding method, properties of individual layers (such as emission, transmission, and reflection) are combined algebraically to yield the overall properties of the combined layers. A typical application of the adding method consists of two opposite unidirectional passes throughout the model atmosphere. The upward pass provides an opportunity to evaluate and merge radiance contributions due to thermal emission. In addition, the upward pass calculates: (a) layer single scattering albedo (ω^N), (b) phase function asymmetry factor, (g^N), which is used to calculate the backscatter fraction, (β), (c) layer reflection and transmission functions R_N and T_N, (d) intrinsic upward and downward fluxes ($F_N^{\pm}$) using the two-stream approximation interfaced with the k-distribution method, (e) beginning of the adding method for composite upward fluxes ($F^{1\pm}$) and reflection (R^+), and layer and merged values of the thermal radiance contributions based upon the parameterizied thermal source function Eqs.(4.42-4.45)

To illustrate an application of the adding method to calculate the actual flux profiles, consider a layered atmosphere shown in Figure (4.3). The upward adding pass begins by adding layer (N-1) to layer (N-2). Subsequent layers are added one at a time until layer (N+2) is reached. The composite upward flux from the combination of (N-2) and (N-1), F_N^{1+}, consists of three contributions (see Figure 4.3):

N+2	R_{N+2}, T_{N+2}, $F_{N+2}^{\pm}$
N+1	R_{N+1}, T_{N+1}, $F_{N+1}^{\pm}$
N	R_N, T_N, $F_N^{\pm}$
N-1	R_{N-1}, T_{N-1}, $F_{N-1}^{\pm}$
N-2	/ / / / / / / / / / / / / / R_{N-2}, F_{N-2}^{+}

Figure 4.3 LOWTRAN 7 Example of the model used for the adding method. R_N and T_N represent the layer N reflection and transmission functions, respectively. $F\pm_N$ is the "local" flux intrinsic to the layer top and bottom for the infrared parame- terization.

52

i. The intrinsic upward flux from layer (N-1), F_{N-1}^+

ii. The multiple reflection of the intrinsic upward flux from layer (N-2), transmitted through layer (N-1), F_{N-2}^+,

$$F_{N-2}^+ T_{N-1} + F_{N-2}^+ T_{N-1} R_{N-1}R_{N-2} + F_{N-2}^+ T_{N-1}(R_{N-1}R_{N-2})^2 + \ldots$$

$$= F_{N-2}^+ T_{N-1}(1 - R_{N-1}R_{N-2})^{-1}$$

(4.56)

where the surface boundary emission is given by:

$$F_{N-2}^+ = F_o^+ = \pi \varepsilon_s B(T_s)$$

(4.57)

and the reflection funtion for (N-2) is

$$R_{N-2} = R_o = (1-\varepsilon_s)$$

(4.58)

and

$$F_{N-2}^-, T_{N-2} = F_o^-, T_o = 0$$

(4.59)

where T_s is the surface temperature and ε_s is the surface emissivity.

iii. The multiple reflection of the intrinsic downward flux from layer (N-1), F_{N-1}^-, reflected from layer (N-2) and transmitted through layer (N-1), i.e.,

$$F_{N-1}^- T_{N-1}R_{N-2} + F_{N-1}^- T_{N-1}R_{N-2}(R_{N-1}R_{N-2}) + \ldots$$

$$= F_{N-1}^- T_{N-1}R_{N-2}(1-R_{N-1}R_{N-2})^{-1}.$$

(4.60)

These will sum to the composite flux:

$$F_{N-1}^+ = F_{N-1}^+ + T_{N-1}(F_{N-2}^+ + F_{N-1}^- R_{N-2})(1 - R_{N-1}R_{N-2})^{-1}.$$

(4.61)

Similar considerations lead to the composite reflection of

layers (N-1) and (N-2):

$$R^+_{N-1} = R_{N-1} + R_{N-2}T^2_{N-1}(1 - R_{N-1}R_{N-2})^{-1}. \qquad (4.62)$$

Next layer (N) is added to the composite of (N-1, N-2), result-ing in composite values for layer N:

$$F^{1+}_N = F^+_N + T_N(F^{1+}_{N-1} + F^-_N R^+_{N-1})(1 - R_N R^+_{N-1})^{-1}$$

$$\qquad\qquad\qquad\qquad\qquad\qquad\qquad (4.63)$$

$$R^+_N = R_N + R^+_{N-1}T^2_N(1 - R_N R^+_{N-1})^{-1}.$$

This process is repeated for layer (N+1):

$$F^{1+}_{N+1} = F^+_{N+1} + T_{N+1}(F^{1+}_N + F^-_{N+1}R^+_N)(1 - R_{N+1} R^+_N)^{-1}$$

$$\qquad\qquad\qquad\qquad\qquad\qquad\qquad (4.64)$$

$$R^+_{N+1} = R_{N+1} + R^+_N T^2_N(1 - R_{N+1} R^+_N)^{-1}$$

and layer (N+2):

$$F^{1+}_{N+2} = F^+_{N+2} + T_{N+2}(F^{1+}_{N+1} + F^-_{N+2}R^+_{N+1})(1 - R_{N+2} R^+_{N+1})^{-1}$$

$$\qquad\qquad\qquad\qquad\qquad\qquad\qquad (4.65)$$

$$R^+_{N+2} = R_{N+2} + R^+_{N+1}T^2_{N+1}(1 - R_{N+2} R^+_{N+1})^{-1}.$$

Since there are no layers above (N+2), the upward composite F^{1+}_{N+2} is identically the actual upward flux, i.e.,

$$F^{2+}_{N+2} = F^{1+}_{N+2}. \qquad (4.66)$$

As is evident from the above discussion, calculated compo-site layer values are required for the evaluation of composite values of subsequent layers. This process was not used in the Eddington modification. Omission of the layer connections became the fatal physical flaw since no accountability of layer interaction was included.

At the termination of the upward pass, the following quantities would have been calculated for each layer and stored for the downward pass: (a) the intrinsic layer values, ω_o^N, R_N, T_N, F_N^-, (b) the composite quantities, F_N^{1+}, R^+, and the non-scattered contribution to emission, E_N^o, where

$$E_N^o = E_N^\pm = (1-T_N)\, J_{SA}^N\, (\pm\mu). \tag{4.67}$$

4.3.4.2 Downward Pass

The downward pass is devoted exclusively to the adding method and stream approximation. In analogy to its upward counterpart, downward composite fluxes, F_N^{1-}, and reflectance functions, R_N^-, are calculated during the unidirectional downward pass. However, in addition, both actual upward and downward fluxes, $F_N^{2\pm}$, are calculated from the composite fluxes and reflection functions.

For the topmost layer the downward contribution is

$$F_{N+2}^- = \pi\varepsilon_{N+2} B(T_{N+2}) \tag{4.68}$$

and the reflection funtion for (N+2) is

$$R_{N+2} = (1-\varepsilon_{N+2})$$
$$F_{N+2}^+ = T_{N+2} = 0 \tag{4.69}$$

Therefore, the actual upward and downward fluxes at the interface of layers (N+1) and (N+2) are:

$$F_{N+1}^{2+} = (\, F_{N+1}^{1+} + F_{N+2}^-\, R_{N+1}^+)(1 - R_{N+2}\, R_{N+1}^+)^{-1}$$

$$F_{N+2}^{2-} = (\, F_{N+2}^{1-} + F_{N+1}^+\, R_{N+2})(1 - R_{N+2}\, R_{N+1}^+)^{-1}. \tag{4.70}$$

At this point, actual upward and downward fluxes are available at the boundaries of layer (N+2). This approach to secure the actual upward and downward fluxes which is radically different from the Wiscombe (1977) procedure where flux continuity is assumed at the layer interfaces i.e., the components G_i and H_i contributing to the upward and downward fluxes are equal. No distinction is made concerning the optical properties of the adjacent layers, whereas, LOWTRAN 7 does distinguish those properties based on the reflectance, transmittance, and composite fluxes.

The actual $(F_{N+1}^{2+}, F_{N+2}^{2-})$ upward and downward fluxes are used to calculate the multiple scattering source function applicable to that level e.g., J_{N+2}^{MS}, using the stream approximation Eq. (4.39). This source function provides the layer contribution to the multiply scattered emission, E_{N+2}^{MS}, and this is added to the thermal contribution, E_{N+2}^{o}, Eq. (4.67) evaluated during the upward pass. Proceeding downward, the composite quantities are first calculated by adding the next layer down to the composite above it, for example, the downward composite flux emerging from layer (N+1) and the corresponding downward composite reflections are:

$$F_{N+1}^{1-} = F_{N+1}^- + T_{N+1}(F_{N+2}^- + F_{N+1}^+ R_{N+2})(1 - R_{N+2} R_{N+1})^{-1}$$

$$R_{N+1}^- = R_{N+1} + R_{N+2}T_{N+1}^2(1 - R_{N+1} R_{N+2})^{-1}.$$

(4.71)

Actual fluxes at the interface of layers (N) and (N+1) are then obtained from the composite values:

$$F_N^{2+} = (F_N^{1+} + F_{N+1}^{1-} R_N^+)(1 - R_n^+ R_{N+1}^-)^{-1}$$

$$(4.72)$$

$$F_{N+1}^{2-} = (F_{N+1}^{1-} + F_N^{1+} R_{N+1}^-)(1 - R_n^+ R_{N+1}^-)^{-1}.$$

For the next layer, N, the procedure is identical, resulting in the composites:

$$F_N^{1-} = F_N^- + T_N(F_{N+1}^{1-} + F_N^+ R_{N+1}^-)(1 - R_N R_{N+1}^-)^{-1}$$

$$(4.73)$$

$$R_N^- = R_N + R_{N+1}^- T_N^2 (1 - R_N R_{N+1}^-)^{-1}.$$

and actual fluxes:

$$F_{N-1}^{2+} = (F_{N-1}^{1+} + F_N^{1-} R_{N-1}^+)(1 - R_{N-1}^+ R_N^-)^{-1}$$

$$(4.74)$$

$$F_N^{2-} = (F_N^{1-} + F_{N-1}^{1+} R_N^-)(1 - R_{N-1}^+ R_N^-)^{-1}.$$

Finally, the procedure terminates at the surface layer (N-2), (N-1) interface where:

$$F_{N-1}^{1-} = F_{N-1}^- + T_{N-1}(F_N^{1-} + F_{N-1}^+ R_N^-)(1 - R_{N-1} R_N^-)^{-1}$$

$$(4.75)$$

$$R_{N-1}^- = R_{N-1} + R_N^- T_{N-1}^2 (1 - R_{N-1} R_N^-)^{-1}.$$

Then the total fluxes become:

$$F_{N-2}^{2+} = (F_{N-2}^{1+} + F_{N-1}^{1-} R_{N-2})(1 - R_{N-2} R_{N-1}^-)^{-1}$$

$$(4.76)$$

$$F_{N-1}^{2-} = (F_{N-1}^{1-} + F_{N-2}^+ R_{N-1}^-)(1 - R_{N-2} R_{N-1}^-)^{-1}.$$

In this last step, the upward surface emission flux, F_{N-2}^+ and reflection function, R_{N-2}, are composite quantities since there are no layers below. This completes the downward pass and the multiply-scattered radiance calculation.

4.3.5 Path Radiance

Path radiance calculations are generated with the combination of the stream approximation (SA), and the multiple scattering source funtion at optical depth, (τ), for a path zenith angle $\cos^{-1}\mu$. For level N, the level source function is given by:

$$J^{SA}_{N(\pm\mu)} \approx [1-\omega^{N}_{o}]B(T_{N}))$$

$$+ \ \omega^{N}_{o} \ / \ \pi \ [F^{\pm 1-}_{N} \ \beta^{N}(\mu g^{n}) + F^{\pm}_{N} \ \beta^{N} \ (\mu \ g^{N})]. \tag{4.77}$$

The first term is due to the non-scattered thermal emission, while the second term is due to multiple scattering. Thus the source function can be written as

$$J^{SA}_{N} = J^{o}_{N} \ (\omega^{N}_{o}, T_{N}) + J^{MS}_{N} \ (\mu, \ \omega^{N}_{o}, \ g_{N}, \ F^{\pm}_{N}) \tag{4.78}$$

where the thermal emission term J^{o}_{N} depends only on local layer properties, and the multiply-scattered term J^{MS}_{N} requires, in addition to local properties, the local fluxes which depend on the overall path properties.

The path radiance or emission with MS is obtained by summing the radiance contributions along a particular path. Evaluation of the multiply-scattered radiance contribution, E^{MS}_{N}, for each layer is accomplished via the adding method, as explained above, on the complementary downward pass where it is merged with the previously calculated non-scattered contributions to obtain the total radiance. Once obtained the radiances

I^+ and I^- will be multiplied by π to produce the isotropic hemispheric flux $F\uparrow$ and $F\downarrow$ for the respective level.

4.3.6 K-distribution Method

The basic problem encountered in the calculation of radiative transfer in low spectral resolution models like LOWTRAN, in the prescence of hazy or cloudy conditions, is the coupling between the processes of scattering and absorption by atmospheric gases and that of cloud/aerosol particles. It is extremely difficult to distinguish the two attenuation effects from one another. The complicated molecular absorption band structure for gases would not allow a rapid line by line frequency integration. However, making certain assumptions about *the line shape* one can calculate from available data the absorption coefficient for gases, $(k_a(\nu))$, versus wavenumber for given temperatures and pressures.

In principle, one can directly employ $k_a(\nu)$ in the radiative transfer equations and obtain the numerical solutions. As pointed out by Arking and Grossman (1972), the only difficulty is the complicated nature of the function $(k_a(\nu))$. A typical band will contain anywhere from several hundred to several thousand lines that must be included to obtain reasonable accuracy.

A solution to this difficulty can be found through the use of the k-distribution function. This method makes use of the

fact that for a homogeneous atmospheric layer, the transmission within a relatively wide spectral interval is independent of the ordering of the value of k_a with respect to wavenumber, but depends upon the fraction of the interval that is associated with a particular value of k_a.

In a homogenous gas layer, the k-distribution function is formally related to the mean transmission function $T_{\Delta v}(u)$,

$$
\begin{aligned}
T_{\Delta v}(u) &= 1/\Delta v \int_{\Delta v} e^{-ku} \, dv \\
&= \int_0^\infty f(k)e^{-ku} \, dk \\
&= \int_0^1 e^{-ku} \, dg \\
&= \sum_1^n e^{-k_i u} \, \Delta g_i
\end{aligned}
\tag{4.79}
$$

where (Δv) is the narrow repeated interval (20 cm^{-1} in LOWTRAN) and (u) is the gas amount. The $f(k)$ for a given gas at a specified Δv is the probability density function such that $f(k)dk$ is the fraction of the frequency interval for which the absorption coefficient is between k and $k+dk$. Eq. (4.80) reveals that the transmission depends on the distribution of the k-values within Δv, but not on the ordering of the values.

The cumulative k-distribution function is $g(k)$ while $(k_i, \Delta g_i)$ are the discrete sets of values to approximate the integral in Eq. (4.80). For lines which are randomly distributed, allowing overlap, and assuming the lines shapes are square, the k-distribution function can be a Poisson distribution according to Arking and Gossman (1972). For example, if

one line contributes an absorption k_o over the interval $2ad$ where (d) is the mean line spacing, then the permitted values are $k_n k_o$, where n is a positive integer, and the k-distribution function is

$$g(k)(k=nk_o) = 2(\alpha)^n e^{-2\alpha/n!}, \quad n=0,1,2,\ldots, \qquad (4.80)$$

Transmission functions for most atmospheric gases and perhaps also at almost all spectral ranges are non-exponential, if derived for spectral intervals of finite width $\Delta\lambda$. The theoretical treatment of radiative transfer in scattering and absorbing media, however, requires strict exponential transmission laws.

This deficiency is overcome by fits of the transmission function (T) to finite sums of exponentials, as defined by

$$T_{\Delta v} (\bar{v}) = \sum_{i=1}^{n} a_i e^{-b_i u}, \qquad (4.81)$$

where $\bar{v}$ is the center wavelength of the interval Δv, and u is the absorbing path length. To obtain physically meaningful terms of this sum, the coefficients a_i and exponents b_i must obey the following conditions:

$$0 \leq a_i \leq 1 , \quad \sum_{i=1}^{n} a_i = 1$$

and

$$b_i \geq 0.$$

The exponents b_i are essentially identical with the volume absorption coefficients (k) and have the dimension of (km^{-1}).

By expressing the band model transmission as the sum of exponentials, the multiple scattering calculation for each

component can be performed independently as if it were a monochromatic problem. Recall, that the optical depth in the infrared parameterization was related to the extinction coefficient by:

$$\tau = k_\nu u + \tau_s (1-g) + \tau_a. \qquad (4.82)$$

This effectively allows differentiation between the aerosol contribution to extinction and gaseous effects of absorption and scattering.

The k-distribution method decouples the band model determined optical properties into a set of equivalent monochromatic calculations which are summed to give the spectrally averaged results. For LOWTRAN 7, the stream approximation is performed through an interface routine consisting of the k-distribution method. This combination of methods, namely the stream approximation and the k-distribution method have been used to study the radiative effects of aerosols (see Hansen et al., 1980). My Eddington modification did not refine the difference between the individual absorption bands for gases but took the extinction coefficients from the inverted transmittances from LOWTRAN 6.

The fitting routine of Wiscombe and Evans (1977) has been used for the two LOWTRAN transmission functions of water vapor /uniformly mixed gases and ozone the primary gaseous absorbers in the troposphere. The accuracy of the fitting is, in general, within a few percent for transmittances greater than 0.1. For inhomogeneous atmospheres, the adopted scaling approximation is

$$k_i(P,T) = k_i(P_o,T_o) \, P/P_o \, \sqrt{(T_o/T)} \qquad (4.84)$$

where T_o, P_o are reference temperature and pressures, respectively.

5.0   PHYSICAL PARAMETERS for the AEROSOL-LADEN BOUNDARY LAYER

5.1   Overview

Armed now with a code which can adequately handle the complexity of multiple scattering, the comparison between multiple and single scattering can proceed. The method of inspection is to use the principle of juxtaposition to elicit the quantified difference between the net fluxes at prescribed levels in a heavily aerosol-laden boundary layer representative of a naturally occurring haze condition. In my experience, this occurs during the summer months under high pressure conditions with a well established inversion trapping aerosols within the lower troposphere. The maximum input of aerosols may be achieved in the vicinity of urban areas where anthropogenic materials are added to the background distribution.

5.2 Model Assumptions

To accomplish my topical objective of quantifying the difference between multiple and single scattering in an aerosol-laden boundary layer, a model representative of an urban, summer time scenario is selected. Such a model is available in the LOWTRAN family of atmospheric models. The overall structure is that of a plane-parallel, cloudless environment

supplemented with a tropical water vapor profile. This model atmosphere is subdivided into 11 levels and ten layers starting at two kilometers and extending downward to the surface which is assumed at sea level. Table 5.1 shows the profile of various parameters applicable to the following discussion.

Several simplifying assumptions are made concerning the model and the method of comparison. 1) Scattering is done only by aerosols. Molecular scattering is ignored. The justification for this lies in the fact that gaseous scattering (Rayleigh scattering) is inversely proportional to the fourth power of the wavelength. Therefore, in the terrestrial infrared domain ($\geq 5.0\mu m$) the effect is negligible. 2) Particle temperature is equal to the medium temperature. 3) Kirchhoff's law applies. This law states a medium may absorb radiation of a particular wavelength, and at the same time also may emit radiation of the same wavelength. The rate at which emission takes place being a function of temperature and wavelength, under the condition of local thermodynamic equilibrium (LTE). In other words, the reduction in the intensity of a pencil of radiation is a consequence of absorption and scattering by the intervening material. However, where absorption is occurring so is emission according to Planck's law of blackbodies. Therefore, the intensity may be strengthened by emission within the line of sight plus multiple scattering from all directions into the line of sight. Symbolically, the above physical processes are represented by:

TABLE 5.1 BOUNDARY LAYER MODEL ATMOSPHERE

L	Z (km)	RH (%)	P (mb)	T (°K)	VIS (km)	E_{t_1} (km^{-1})
1	2.000	100.0	802.0	289.7	0.55	7.06
2	1.750	97.3	826.2	286.4	0.83	4.78
3	1.500	95.2	850.9	287.6	1.15	3.41
4	1.250	92.9	876.1	288.6	1.53	2.51
5	1.000	91.1	920.0	289.6	1.94	2.01
6	0.750	88.9	928.6	290.8	2.46	1.59
7	0.500	88.2	955.9	291.9	2.96	1.32
8	0.250	87.3	984.1	293.0	3.47	1.12
9	0.100	86.7	1001.3	293.7	3.79	1.01
10	0.050	86.4	1007.1	294.0	3.89	0.99
11	0.001	86.2	1012.9	294.2	3.99	0.97

Z = elevation of level L in (km)

RH = relative humidity at level L

P = pressure at level L

T = temperature at level L

VIS = meteorolgical range ($3.912/E_t$)

E_t = extinction coefficient normalizied at $0.55\mu m$

$$j_\nu = k_\nu \, B(T) \qquad\qquad (5.1)$$

where j_ν is the source function coefficient and k_ν is the mass extinction cross section (the sum of the mass absorption and scattering cross section) both coefficients having the same physical meaning. 4) The visibility in my model decreases with height to reach its minimum at the top of the inversion layer. Correspondingly, the *extinction coefficient* increases to reach its maximum at the same location. This model adjustment is selected to mimic summertime conditions in an urban environment where, in the presence of an inversion and strong insolation, convective "boiling" and vertical turbulent transport differentially mix the particulate matter with lowest visibilities found immediately below the inversion, as described in a model by Venkatram and Viskanta (1977). 5) The number concentration is fixed at 2.0×10^4 particles/cm^3. However, particle size increases with increasing humidification. This is a LOWTRAN artifact which relates the meteorological range to the layer relative humidity based on extensive research conducted by Hanel (1972, 1976) and McClatchey et al. (1972). dependent configuration. It is intented only to quantify the difference of multiple and single scattering allowing only the transfer of radiant energy to occur over the same environmental conditions.

5.3   Urban Aerosol Characteristics

Urban atmospheric aerosols and their radiation absorption and scattering properties are characterized by their size dis-

tribution, chemical composition, and physical properties such as density and the complex index of refraction. The urban aerosol can be separated into distinct groups based on their size and chemical composition according to Viskanta and Weirich (1979). The first group consists generally of particles with radii greater than 2μm. These particles are composed primarily of silicon oxides with substantial amounts of calcium and lesser amounts of iron oxides and metal chlorides. The second group consists generally of particles which have radii less than 2μm. These particles are chiefly anthropogenic in origin and are either produced directly as aerosol or by heterogeneous nucleation of gas-phase pollutants. Chemical analysis of these particles shows large concentrations of sulfur and carbon compounds with varying amounts of lead, zinc, arsenic, and other metals.

The urban aerosol model in LOWTRAN 7 is a combination of the rural aerosol, composed of a mixture of 80 percent of water soluble substance (ammonium and calcium sulfate and also organic compounds), and 20 percent sootlike, carbonaceous aerosols. The sootlike aerosols are assumed to have the same size distribution as the other components according to Shettle and Fenn (1979). Because of the hygroscopic nature of the many chemical compounds which make up the urban aerosol and the presence of high humidities in urban areas at mid-latitudes in the summer, the particles are often composed largely of liquid water. This then leads to water coated particles which are com-

posite spheres containing several individual constituents. Figure (5.1) shows a visual presentation of this process. Since the volume increases by the cube of the radius, the fraction of water also increases rapidly when the air humidity increases. This means that the Mie theory for spherical particles will be more accurate the higher the air humidity is and also that the refractive index (real portion) approaches the value of liquid water (1.33).

5.4 Humidification Effects on Aerosol Properties

As indicated above, the urban aerosols being hygroscopic in nature are subject to changes in their physical properties as the ambient relative humidity increases. Water vapor condensing out of the atmosphere onto particulates suspended in such an atmosphere tends to swell their size and change their composition thus their effective complex refractive index. The resulting effect of the aerosols on the absorption and scattering of light will correspondingly be modified.

The change in particle size is related to the relative humidity by an equation developed by Hanel (1976):

$$r(a_w) = r_o[1 + \rho\, m_w(a_w/m_o]^{1/3} \tag{5.2}$$

where r_o is the dry particle radius, ρ is the particle density relative to that of water, m_o is the dry particle mass, $m_w(a_w)$ is the mass of the condensed water, and (a_w) is the water activity which is essentially the relative humidity (f),

1. Dry particle (RH = 0 %)

water soluble substances, density = δ_s

water insoluble substances, density = δ_i

radius = r_o

fraction of water soluble substances = E

2. Droplet (RH = 80 %)

salt solution, density = δ'

water soluble substances, density = δ_s

water insoluble substances, density = δ_i

radius = r

dissolved fraction of E = ϵ

3. Droplet (RH > 95 %)

salt solution, density = δ'

water insoluble substances, density = δ_i

radius = r

$\epsilon = 1$
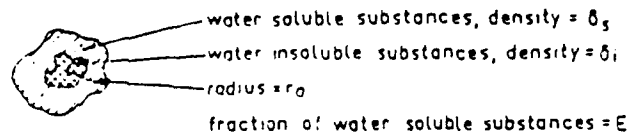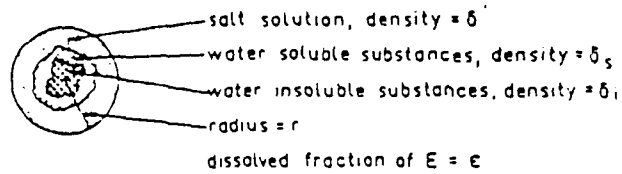
Figure 5.1 An aerosol particle model which shows an increase in radius (r) and change in the fraction of water soluble and water insoluble substances (ϵ) as the relative humidity increases in the environment refelcted in the densities $\delta_{i,s}$ (after Nilsson, 1979).

corrected for the curvature of the particle surface, vis.,

$$a_w = f \exp(-2\sigma V_w / R_w T r),$$ (5.3)

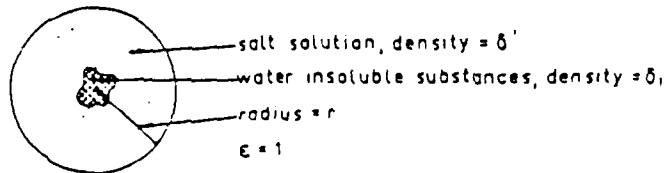where σ is the surface tension on the wet particle surface, V_w is the specific volume of water, R_w is the specific gas constant for water, and T is the absolute temperature.

Once the wet aerosol particle size is found from Eqs (5.1 and 5.2), the effective complex refractive index for composite water coated substances becomes the volume weighted average of the refractive indexes of the dry aerosol substance, n_o and water n_w. Equivalently, this can be written as (after Hanel, 1976):

$$n = n_w + (n_o - n_w)[r_o / r(a_w)]^3.$$ (5.4)

Figure (5.2) shows the real and imaginary parts of the complex refractive index as a function of wavelength for an urban aerosol collected in a study by Nilsson, (1979). The real part decreases when the humidity increases except around 3.15μm and 8.2μm. This is particularly noticeable for wavelengths greater than 9.0μm. The imaginary part has a pronounced peak at 9.2μm caused by absorption in quartz, silicon, and ammonium sulfate. This peak decreases when the air humidity increases simultaneously as peaks caused by absorption in water, grow at 2.95μm, 6.0μm, and 15-20μm. Greater absorption of electromagnetic energy by the water substance (vapor and liquid) in the above opaque spectral bands is indicated by the increasing values of the imaginary portion of the complex index of refraction. Thus
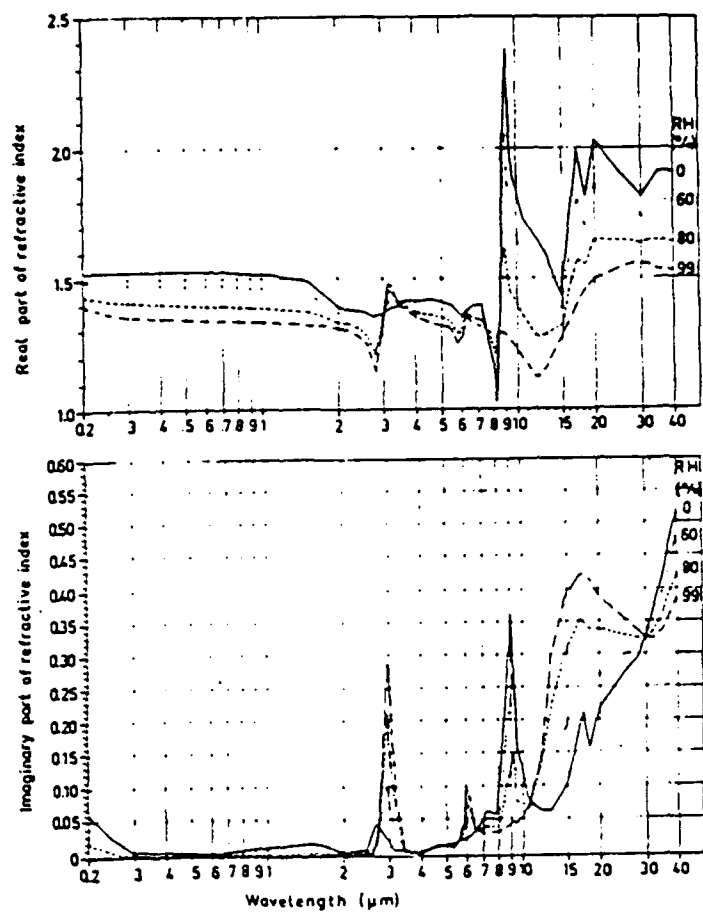
Figure 5.2 The real and imaginary parts of refractive index for aerosol partilces as a function of wavelength at different relative humidities for an urban aerosol collection (after Nilsson, 1979).

72

more energy will internalized by the intervening water vapor and water coated aerosols. This reduces the probability that the scattering and refraction processes will contribute to the diffuse radiation field. However, increased absorption leads to a concurrent greater emission from the intervening medium. Therefcre, the "true creation" of photons, a direct contribution, would enhance the total flux density field. These physical phenomenon are intertwined in a complex manner in a model where the visibility is tied to the relative humidity. The change of the complex refractive index along with the increasing size of the particles as the humidity approaches saturation effectively changes the extinction coefficient (the combination of scattering and absorption bulk properties described in Chapter 3). This in turn effects the meteorological range (V) given by the Koschmieder formula

$$V = 1/\beta \ \ln 1/\varepsilon = 3.912/\beta \qquad\qquad (5.5)$$

where (β) is the extinction coefficient, and (ε) is the threshold contrast, set equal to 0.02. As used in LOWTRAN, the inputs for visibility are in terms of meteorological range, with (β) evaluated at 0.55μm.

The meteorological ranges presented in Table (5.1) come from the Army Vertical Structure Algorithm (VSA) build into LOWTRAN 7. This is a subprogram which effectively subdivides the model boundary layer into a finer resolution. The VSA allows various prescriptions for the aerosol configurations to include the heavy haze condition (case 2) which forms the basis

of my heavily aerosol-laden test case.

5.5 Relative Fractional Comparisons and Net Flux Generation

LOWTRAN 7 is run in the radiance mode to calculate the difference between multiple and single scattering. This is accomplished by toggling between the two available modes currently installed. The method of comparison is then to find the net fluxes (F_{net}) for each scattering configuration at set levels and compare the relative fractional difference (reldiff) given by:

$$(MS-SS)/SS \qquad (5.6)$$

where MS is the multiply scattered net flux values and SS is the singly scattered net flux.

To calculate the net fluxes (F_{net}) at each level the respective upward and downward radiances ($I\uparrow$ and $I\downarrow$) must be known. The net flux (F_{net}) is related to these by the simple relationship

$$F_{net} = \pi \ (I\uparrow - I\downarrow) \qquad (5.7)$$

based on the isotropy conditions in the thermal radiation fields. Here the downward radiance ($I\downarrow$) is chosen as subtrahend since it is expected that the upward radiance at each level will be larger since the highest temperatures are located in the lowest levels of the boundary layer. Thus, emission would be larger looking downw. ..

The upward radiances are calculated by looking down toward the surface from each successive preestablished level starting at two kilometers. The surface boundary conditions are a surface temperature(T_s) of 300°K and surface emissivity (ε) of 0.85. These values are selected to mimic mid-latitude summertime conditions and a combination of rural and urban landscapes as suggested by Goody (1964).

The LOWTRAN 7 program is set to move through the levels once for each of 34 wavenumber intervals beginning at 350 cm^{-1} to 2000 cm^{-1} at 50 cm^{-1} steps. This is done to generate a spectrally sensitive output which reflects the absorption and emission characteristics of the radiatively active constituents in the test model. An angular dependence is set by looking down at zenith angles of 180°, 140°, and 120°.

The downward radiances (I↓) are calculated by looking up toward the top of the boundary layer (2 kms) with the exception that the first downward radiance is a composite of the intervening layers from 20.0 kms. Successive downward radiance calculations occur at each level in the boundary layer again varying the zenith angle, looking up, at 0°, 40°, and 60° then over same spectral intervals.

Each respective level up and down radiance is then multiplied by π to produce the hemispheric isotropic flux. Assuming isotropy for these fluxes is consistent with the type of radiant emission from layers under LTE. This is again a basic assumption pertinent to my study. Now that the fluxes are

available Eq. (5.5) can be used to calculate the net fluxes (F_{net}).

The relative fractional difference is produced using the net fluxes at each level for each type of scattering mode (SS or MS) with comparisons being made over zenith angle (θ) and wavenumber interval (Δv). The formulation appears as:

$$Reldif(\theta, \Delta v) = [Fnet^{MS}(\theta, \Delta v) - Fnet^{SS}(\theta, \Delta v)]$$
$$/ \ Fnet^{SS}(\theta, \Delta v). \tag{5.8}$$

The information from Eq. (5.7) provides insight about the quantified difference between MS and SS in a heavily aerosol-laden boundary layer environment.

6.0 Interpretation of Results

6.1 Overview

Careful examination of the output data revealed several distinct trends in regards to the behavior of the relative fractional difference (Reldiff) and particular spectral regions. It is evident that the distinction between multiple scattering (MS) and single scattering (SS) is practically zero for those wavenumber regions where strong water vapor absorption is occurring. Uniformly, over all zenith angles, this trend repeated itself at elevations in the boundary layer where the relative humidities exceeded 88% (level 7, 0.50 km). In these same spectral regions it is found that, below level 7, negative MS net fluxes ($F\uparrow - F\downarrow$), downward directed net flux, dominate by as much as 40 times the SS net fluxes. Another finding is that for "window regions" in the infrared portion of the spectrum, which are much less opaque to thermal radiation, the MS net fluxes exceed the SS net fluxes at all levels and increases to a maximum as the zenith angle increases. Therefore, since the above trends are found throughout the data, the presentation for the interpretation of results will be limited to two representative spectral bands, as numerically exemplified by the 1650 cm^{-1} (6.1μm) and 950 cm^{-1} (10.5μm) wavenumbers.

77

6.2   Atmospheric Effect and the Thermal
      Infrared Spectrum

Certain portions of the infrared radiation spectrum are absorbed by various gases in the atmosphere. Among these gases, carbon dioxide, water vapor, and ozone are the most important. Figure 6.1 shows the emission spectrum for a surface temperature of 295°K. Strong absorption is found due to water vapor in the 6.3μm band from about 1200 to 2000 cm^{-1} and in the rotational bands below 600 cm^{-1}. Except for ozone, which has an absorption band in the 1040 cm^{-1} (9.6μm) region, the atmosphere is relatively transparent from 800 to 1200 cm^{-1}. This region is referred to as the "atmospheric window." It is seen from Figure 6.1 that the choice for the 1650 cm^{-1} band places it squarely in the middle of the strongest H_2O absorption. Whereas, the 950 cm^{-1} band is selected to be outside the ozone (O_3), carbon dioxide (CO_2), and water vapor (H_2O) bands.

6.3   The 1650 cm^{-1} (6.0μm) Absorption Band

The 1650 cm^{-1} absorption band comparisons of MS versus SS fluxes are shown in Table 6.1 through 6.3. These results show that regardless of the viewing angle above 0.25 km (levels 1 through 7) the difference between MS and SS net fluxes are eradicated. My interpretation of this result is that water vapor plus liquid water coated aerosol absorption is so great that any distinction between the scattering processes are completely negated.
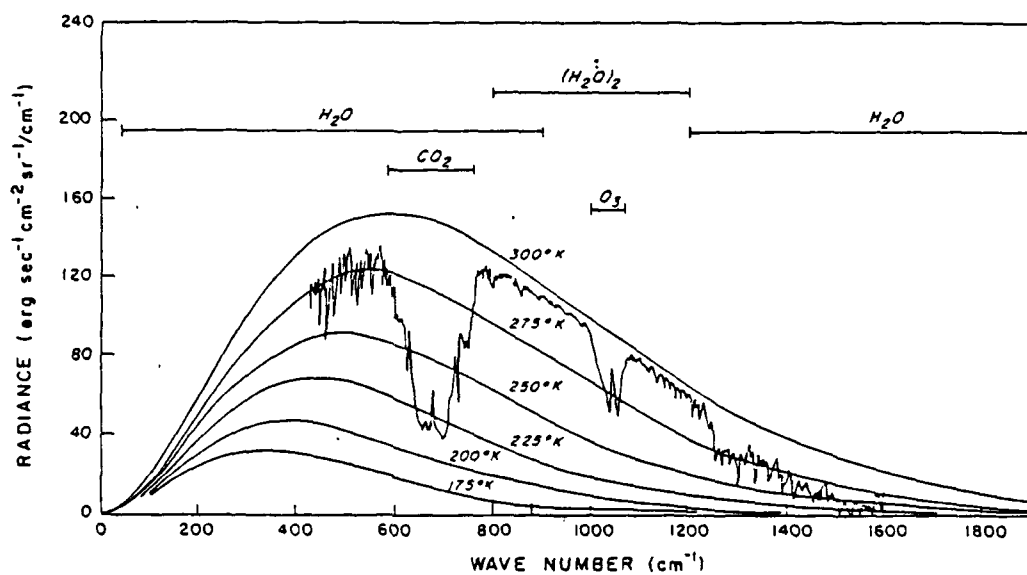
Figure 6.1 The terrestrial infrared spectra and various absorption bands. Also shown is an actual atmospheric emission spectrum taken by the Nimbus IV IRIS instrument near Guam at 15.1 N and 215.3 W (after Liou, 1980).

TABLE 6.1: 1650 cm^{-1} ABSORPTION BAND
ZENITH ANGLES 0° and 180°

L	SS	MS	Reldiff
1	0.9400E-07	0.9400E-07	0.0000
2	0.3100E-07	0.3100E-07	0.0000
3	0.6300E-07	0.6300E-07	0.0000
4	0.9400E-07	0.9400E-07	0.0000
5	0.9400E-07	0.9400E-07	0.0000
6	0.9400E-07	0.9400E-07	0.0000
7	0.1260E-06	0.1260E-06	0.0000
8	0.1570E-06	-.5027E-05	-33.02
9	0.1260E-06	-.5089E-05	-41.39
10	0.1570E-06	-.5088E-05	-33.41
11	0.1250E-06	-.2526E-05	-21.21

L : level number

SS = Fnet^{SS} : the single scattered net flux at level L

MS = Fnet^{MS} : the multiple scattered net flux at level L

Reldiff : relative fractional difference between the
net fluxes (MS-SS) / SS

TABLE 6.2: 1650 cm^{-1} ABSORPTION BAND
ZENITH ANGLES 40° and 140°

L	SS	MS	Reldiff
1	0.9400E-07	0.9400E-07	0.0000
2	0.3100E-07	0.3100E-07	0.0000
3	0.6300E-07	0.6300E-07	0.0000
4	0.9400E-07	0.9400E-07	0.0000
5	0.9400E-07	0.9400E-07	0.0000
6	0.9400E-07	0.9400E-07	0.0000
7	0.1260E-06	0.1260E-06	0.0000
8	0.1570E-06	-.5027E-05	-33.02
9	0.1260E-06	-.5089E-05	-41.39
10	0.1570E-06	-.5089E-05	-33.41
11	0.1250E-06	-.1885E-05	-16.08

L : level number

SS = Fnet^{SS} : the single scattered net flux at level L

MS = Fnet^{MS} : the multiple scattered net flux at level L

Reldiff : relative fractional difference between the
net fluxes (MS-SS) / SS

TABLE 6.3: 1650 cm^{-1} ABSORPTION BAND
ZENITH ANGLES 60° and 120°

L	SS	MS	Reldiff
1	0.6300E-07	0.6300E-07	0.0000
2	0.3100E-07	0.3100E-07	0.0000
3	0.6300E-07	0.6300E-07	0.0000
4	0.9400E-07	0.9400E-07	0.0000
5	0.9400E-07	0.9400E-07	0.0000
6	0.9400E-07	0.9400E-07	0.0000
7	0.1260E-06	0.1260E-06	0.0000
8	0.1570E-06	-.5027E-05	-33.02
9	0.1260E-06	-.5089E-05	-41.39
10	0.1570E-06	-.5089E-05	-33.41
11	0.1250E-06	-.1884E-05	-15.83

L : level number

SS = Fnet^{SS} : the single scattered net flux at level L

MS = Fnet^{MS} : the multiple scattered net flux at level L

Reldiff : relative fractional difference between the
        net fluxes (MS-SS) / SS

Sensibly, this incorporates the notion that as the relative humidities increase the size of the aerosol particles would increase. Therfore, an increasing amount of liquid water is needed to encapsulate the originally drier particle. This in turn changes the complex index of refraction to higher imaginary values as pointed out in Figure (5.2). Appropriately, this allows more absorption to occur within those layers where the relative humidities are high enough to trigger the effect. This is graphically depicted in Figure 6.2 which is a plot of the partial aerosol extinction coefficients (absorption and scattering) at 50% and 99.8% relative humidities (RH) for an urban aerosol which is similar in number density, composition, and size distribution used in my investigation. At the 99.8% RH at wavenumber 6.0μm the scattering and absorption coefficients are approximately equal. However, closer inspection shows that the scattering extinction coefficient (E_s) for this spectral band is decreased and the absorption extinction coefficient (E_a) increases to a maximum around 15.0μm. This shows, indirectly, that the probability increases that a photon emitted or scattered (by either process) would be almost instantaneously absorbed. In addition, analysis of the up and down fluxes for each angle showed that the differences between them is minimal for both MS and SS (10^{-7}) at levels where the RHs exceeded 88% (see Table 6.4 for a representative example). This indicates that isotropic thermal emission (evenly distributed up and down fluxes) is occurring in those layers and that any directionality due to scattering, implicitly present in the

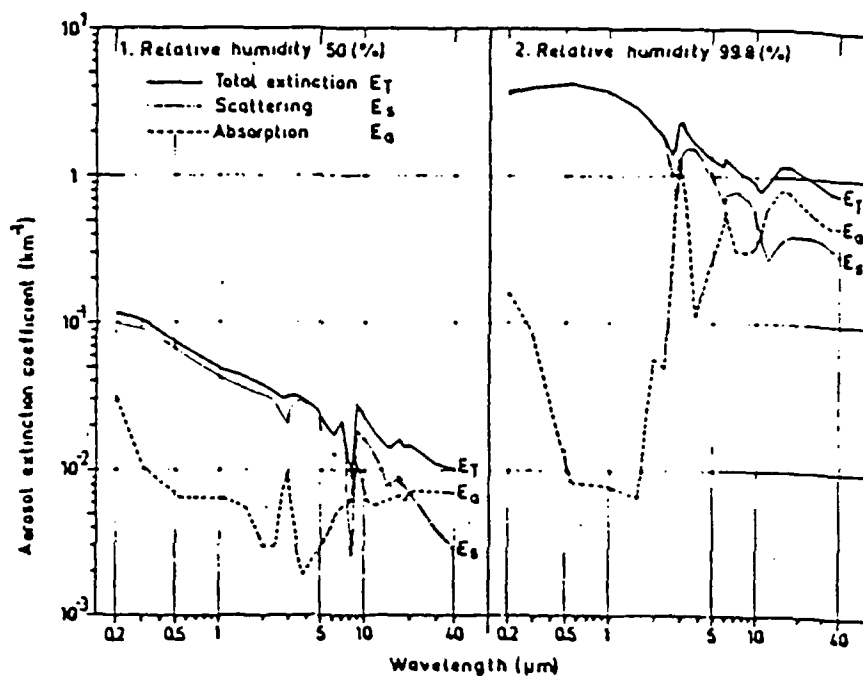Figure 6.2   The total (E_T) and partial extinction   coefficients
as a function of wavelength for the scattering (E_s) and absorp-
tion (E_a) fractions at 50% and 99.8% RH. Aerosol size distribu-
tion from urban sample (after Nillson, 1979).

TABLE 6.4: 1650cm^{-1} REPRESENTATIVE MULTIPLE and SINGLE SCATTERING UP and DOWN FLUXES at ZENITH ANGLE 40°

Multiple Scattering

Level	down-flux	up-flux	net-flux
1	0.4304E-05	0.4398E-05	0.9400E-07
2	0.4210E-05	0.4241E-05	0.3100E-07
3	0.4335E-05	0.4398E-05	0.6300E-07
4	0.4461E-05	0.4555E-05	0.9400E-07
5	0.4618E-05	0.4712E-05	0.9400E-07
6	0.4775E-05	0.4869E-05	0.9400E-07
7	0.4838E-05	0.4964E-05	0.1260E-06
8	0.5027E-05	0.2099E-18	-.5027E-05
9	0.5089E-05	0.3770E-12	-.5089E-05
10	0.5089E-05	0.1784E-09	-.5089E-05
11	0.5121E-05	0.3236E-05	-.1885E-05

Single Scattering

Level	down-flux	up-flux	net-flux
1	0.4304E-05	0.4398E-05	0.9400E-07
2	0.4210E-05	0.4241E-05	0.3100E-07
3	0.4335E-05	0.4398E-05	0.6300E-07
4	0.4461E-05	0.4555E-05	0.9400E-07
5	0.4618E-05	0.4712E-05	0.9400E-07
6	0.4775E-05	0.4869E-05	0.9400E-07
7	0.4838E-05	0.4964E-05	0.1260E-06
8	0.5027E-05	0.5184E-05	0.1570E-06
9	0.5089E-05	0.5215E-05	0.1260E-06
10	0.5089E-05	0.5246E-05	0.1570E-06
11	0.5121E-05	0.5246E-05	0.1250E-06

85

backscatter fraction (β) for MS (0.15 from Figure 4.2) and the asymmetry factor (g) (.8520 from Shettle and Fenn, 1979), is extinguished. The overall effect is rapid re-absorption and re-emission which masks out any contribution by aerosol scattering.

The sudden appearance of the MS net downward fluxes at levels eight through eleven (present in Tables 6.1-6.3) is explained in conjunction with the ideas presented above. In these cases, the MS scattering process supercedes absorption and establishes a directional character. So much so as to overwhelm the SS process by 40 times! This notion is supported by Figure 6.2 with emphasis now shifted to the 50% RH graph. In this case the scattering extinction coefficient (E_s) is much larger for 6.0μm than the absorption coefficient (E_a). This indicates a trend whereby as the RHs decrease, even marginally, the MS process with its favored downward directionality is able to produce much larger flux densities due to the presence of aerosols. The fact that those layers above, when combined together, are by nature much thicker ensures a much larger out-put of photons in the downward direction. This idea is sup-ported again by inspection of the downward and upward fluxes for each process. In each angular case the MS down fluxes overwhelmed the up fluxes by eight orders of magnitude at all levels greater than seven (see Table 6.4). Here it can be seen that the difference of the SS fluxes do not change appreciably showing conclusively the directional nature the MS flux.

6.4 The 950 cm^{-1} (10.5μm) Window Region

Tables 6.5 through 6.7 present the net flux differences for the 950cm^{-1} window region. In this spectral domain, absorption by the principal infrared absorbing gases is greatly reduced. Therefore, a comparison of MS and SS fluxes can be presented with absorption considerations minimized. Several trends are noted: First, positive upward net fluxes dominated over negative downward net fluxes for all zenith angles and elevations. Second, multiple scattering (MS) produces larger positive net fluxes than single scattering (SS) over all elevations with an increasing difference between the two being found as the zenith angle (θ) increases. Third, for both SS and MS, the positive flux densities increase as the level elevation from the surface becomes greater. Fourth, a downward trend is seen for positive flux densities for both MS and SS as the geometric path length expands due to secant elongation.

The positive upward fluxes are expected, now, since in this spectral regime thermal emission for terrestrial temperatures is approaching a maximum and such emission from lower elevations at higher temperatures is capable of being transmitted to the levels above. A cumulative effect occurs as the concatenation of levels takes place. Thus, a straight downward looking sensor would "see" larger flux density values as the distance between the surface and the sensor increased. This is similar to what happened with the immense downward flux found in the strong absorption band. The preponderance of emitted

TABLE 6.5: 950 cm^{-1} WINDOW BAND
ZENITH ANGLES 0° and 180°

L	SS$_{Fnet}$	MS$_{Fnet}$	Reldiff
1	0.2532E-04	0.2670E-04	0.0545
2	0.2413E-04	0.2695E-04	0.1169
3	0.2143E-04	0.2485E-04	0.1596
4	0.1935E-04	0.2321E-04	0.1995
5	0.1766E-04	0.2177E-04	0.2327
6	0.1618E-04	0.2030E-04	0.2546
7	0.1480E-04	0.1923E-04	0.2993
8	0.1341E-04	0.1505E-04	0.1223
9	0.1260E-04	0.1596E-04	0.2667
10	0.1232E-04	0.1643E-04	0.3263
11	0.1200E-04	0.1687E-04	0.4058

L : level number

SS = Fnet^{SS} : the single scattered net flux at level L

MS = Fnet^{MS} : the multiple scattered net flux at level L

Reldiff : relative fractional difference between the
net fluxes (MS-SS) / SS

L	SS	MS	Reldiff
1	0.2441E-04	0.2554E-04	0.0463
2	0.2287E-04	0.2567E-04	0.1224
3	0.1964E-04	0.2313E-04	0.1777
4	0.1725E-04	0.2117E-04	0.2272
5	0.1536E-04	0.1954E-04	0.2721
6	0.1373E-04	0.1807E-04	0.3161
7	0.1219E-04	0.1684E-04	0.3815
8	0.1075E-04	0.1172E-04	0.0902
9	0.9860E-05	0.1300E-04	0.3185
10	0.9520E-05	0.1357E-04	0.4254
11	0.9230E-05	0.1429E-04	0.5482

L : level number

SS = Fnet^{SS} : the single scattered net flux at level L

MS = Fnet^{MS} : the multiple scattered net flux at level L

Reldiff : relative fractional difference between the
net fluxes (MS-SS) / SS

TABLE 6.7: 950 cm^{-1} WINDOW BAND
ZENITH ANGLES 60° and 120°

L	SS$_{Fnet}$	MS$_{Fnet}$	Reldiff
1	0.2259E-04	0.2310E-04	0.0226
2	0.2026E-04	0.2300E-04	0.1352
3	0.1612E-04	0.1976E-04	0.2202
4	0.1335E-04	0.1728E-04	0.2944
5	0.1124E-04	0.1543E-04	0.3728
6	0.9550E-05	0.1385E-04	0.4503
7	0.8020E-05	0.1244E-04	0.5511
8	0.6530E-05	0.5880E-05	0.0902
9	0.5620E-05	0.8050E-05	0.4324
10	0.5280E-05	0.8920E-05	0.6894
11	0.4960E-05	0.1011E-04	1.0383

L : level number

SS = Fnet^{SS} : the single scattered net flux at level L

MS = Fnet^{MS} : the multiple scattered net flux at level L

Reldiff : relative fractional difference between the
net fluxes (MS-SS) / SS

photons is so large as to overwhelm the downward directionality inherent in the aerosol particles which intercept the upwelling radiation.

Another subtle physical process is at work which effects the number density of the aerosols as the zenith angle increases. The overall effect is for both MS and SS positive net fluxes (with MS positive fluxes still bigger) to decrease as the geometric path length is increased due to secant path elongation. The angular dependence is interpreted as effect of a secant stretching whereby the geometric path length is increased by

$$\text{Path length} = s \ (1/\cos\theta) \tag{6.1}$$

where (s) is the vertical distance between levels and (θ) is the zenith angle. For example, the path length from the surface to 2.0 km looking at a 40° zenith angle becomes 2.6 km. Obviously, more scatterers will be included in the attenuation process to reduce the flux densities. But MS effects redirect photons back into the impinging pencil to increase over and above the SS process, which for LOWTRAN is a loss mechanism with no self-illumination. However, this process cannot continue without abatement because of particle shadowing.

The phenomenon of particle shadowing occurs when the number of intervening scatters along a path increases to such an extent that the physical separation between particles is greatly reduced from the perspective of traversing photon. Or put another way, the total volume of the scatters increases

within a column to the point where the scattered light from one particle is physically blocked by the presence of another. The opacity of such a path is greater and the flux densities would be reduced. Therefore, in the window region, increasing the number density of aerosol particles along a path will increase the diffuse component, when compared to first order scattering, but then it too is reduced as the particles get in the shadow of other adjacent particles.

7.0 CONCLUSIONS

7.1 Summary of Investigation

The results of this investigation make it obvious that multiple scattering by aerosols of terrestrial infrared radiation is not without consequence. In juxtaposition over the same urban planetary boundary layer model (PBL) the multiply scattered total flux densities (MS), which involves scattering plus emission, are larger than singly scattered total flux densities (SS). This result is especially evident in the absorption band for water vapor (1200 cm^{-1} to 2000 cm^{-1}) where multiple scattering overwhelms single scattering by as much as 44 times (4,400%) in the lowest one third of the PBL. These vastly increased total flux densities are associated with water vapor and water coated aerosol emission emanating from the overlaying two thirds of the PBL where the visibilities are the lowest ($\leq$ 3.0 km) and the relative humidities are the highest ($\geq$ 88.0%). In the water vapor window portion of the infrared spectrum (830 cm^{-1} to 1250 cm^{-1}), thermal emission from the surface is able to penetrate to the top of the urban PBL. Here, the relative fractional difference (MS - SS) / SS, is reduced but MS still is numerically superior ranging from 0.02 to 1.02 times (2% to 102%) the SS flux densities.

In the window region at all levels the net flux densities remain positive (F_{net} = F↑ - F↓) for both single and multiple scattering processes. However, the distinction between the two diminishes with height as shown in Tables 6.5 to 6.7. This result occurs because particle shadowing is reduced allowing the multiple scattering process to dominate. This distinction in the lower levels is enhanced as the zenith angle is increased. This effect is caused by an increase in aerosol number density produced by secant path elongation. From the results it may be inferred that only at the lower levels ($\leq$ 0.25 km) multiple scattering would enhance the positive flux densities and aid in the thermal emission from the surface.

In the absorption bands of water vapor, negative total flux densities (F_{net} = F↑ - F↓) predominate in the lowest one third of the PBL. Here, water vapor and water coated aerosol emission enhanced a downward directed atmospheric counter radiation as shown by the Tables 6.1 through 6.3. The appearance of negative flux densities below 0.50 km leads to the inference that absorption of photons is almost instantaneous and completely masks any scattering process. It may, however, also be inferred that in those levels where water vapor absorption is less critical the scattering process dominates and the "cascade" of photons produced by numerous reabsorptions and reemissions from the layers above is released. The photons are directed downward by the aerosols that favor forward scattering. When of an urban nature the aerosols have an asymmetry

factor of 0.85 and a backscatter fraction (β) of 0.15. It is concluded from these results that a synergistic relationship between absorption/emission and multiple scattering among the radiatively active gases and the aerosol is established, which produces an enhanced total downward directed flux that may aid in heating the lowest layers in an aerosol-laden PBL.

7.2 Suggested Future Research

The results of this investigation suggest that in the absorption bands of water vapor, in the presence of heavily aerosol-laden atmospheric structures, a greatly enhanced total downward directed net flux is produced.

The anonymous flux occurs at levels where the scattering process is able to dominate water vapor absorption. A recommendation is made to study the possible influence this strengthened negative net flux would have on the temperature patterns within a PBL. This could be done by calculating the total flux divergence (ΔF_{net}) at levels located within the PBL and calculating the radiative temperature changes by using the enthalpy rate equation presented by Liou (1980) as

$$\partial T/\partial t = (-1/C_p \rho)\ (\Delta F_{net}/\Delta z). \qquad (7.1)$$

Infrared heating of this nature could play a role in a nocturnal destablization of the lowest portion of the PBL.

REFERENCES

JOURNAL ARTICLES

Ackerman, T.P., K. Liou, and C.B. Leovy, 1975: Infrared Radiative Transfer in Polluted Atmospheres. J. Appl. Meteor., 15, 28-35.

Arking, A., and K. Grossman, 1972: The Influence of Line Shape and Band Structure on Temperatures in Planetary Atmospheres. J. Atmos. Sci., 29, 937-949.

Coakley, Jr., J.A., and R.D. Cess, 1982: The Effect of Tropospheric Aerosols on the Earth's Radiation Budget: A Parameterization for Climate Models. J. Atmos. Sci., 40, 116-138.

Dave, J.V., 1981: Transfer of Visible Radiation in the Atmosphere. Atmos. Env., 15, 1805-1820.

Hanel, G., 1976: The Properties of Atmospheric Aerosol Particles as Functions of the Relative Humidity at Thermodynamic Equilibrium with the Surrounding Moist Air. Advances in Geophysics, 19, 73-188.

Hanel, G., 1972: Computation of the Extinction of Visible Radiation by Atmospheric Aerosols Particles as a Function of the Relative Humidity, Based upon Measured Properties. Aerosol Sci., 3, 377-386.

Hansen, J.E., 1969: Exact and Approximate Solutions for Multiple Scattering by Clouds and Hazy Planetary Atmospheres. J. Atmos. Sci., 26, 478-487.

Hansen, J.E., and L.D. Travis, 1974: Light Scattering in Planetary Atmospheres. Space Sci. Rev., 16, 527-610.

Hansen, J.E., A.A. Lacis, P. Lee, and W.-C. Wang, 1980: Climatic Effects of Atmospheric Aerosol. Aerosols: Anthropogenic and Natural Sources and Transport. Ann. N.Y. Acad. Sci., 383, 575-587.

Joseph, J.H., W.J. Wiscombe, and J.A. Weinman, 1976: The Delta-Eddington Approximation for Radiative Flux Transfer. J. Atmos. Sci., 33, 2452-2459.

Liou, K., 1973: A Numerical Experiment on Chandrasekhar's Discrete-ordinate Method for Radiative Transfer: Application to Cloudy and Hazy Atmospheres. J. Atmos. Sci., 30,

1303-1326.

Meador, W.E., and W.R. Weavor, 1979: Two-Stream Approximations to Radiative Transfer in Planetary Atmospheres: A Unified Description of Existing Models and a New Improvement. J. Atmos. Sci., 37, 630-643.

Nilsson, B., 1979: Meteorological Influence on Aerosol Extinction in the 0.2μm - 40μm Wavelength Range. Applied Optics, 18, 3457-3473.

Schuster, A., 1905: Radiation Through a Foggy Atmosphere. Ap. J. Optics, 21, 1-22.

Schwarzschild, K., 1906: On the Equilibrium of the Sun's Atmosphere. Nachr. Gesell. Wiss. Gottingen, Math.-Phys. Kl., 195, 41-53.

Shettle, E.P., and J.A. Weinman, 1970: The Transfer of Solar Irradiance Through Inhomogeneous Turbid Atmospheres Evaluated by Eddington's Approximation. J. Atmos. Sci., 27, 1048-1055.

Venkatram, A., and R. Viskanta, 1977: Radiative Effec's of Elevated Pollutant Layers. J. Appl. Meteor., 16, 1256-1272.

Viskanta, R., R.W. Bergstrom, and R.O. Johnson 1977: Radiative Transfer in a Polluted Urban Planetary Boundary Layer. J. Atmos. Sci., 34, 1091-1103.

Wang, W., and G.A. Domoto, 1974: The Radiative Effect of Aerosols in the Earth s Atmosphere. J. Appl. Meteor., 13, 521-534.

Welch, R. ai.d W. Zdunkowski, 1976: A Radiation Model of the Polluted Atmospheric Boundary Layer. J. Atmos. Sci., 33, 2170-2184.

Wiscombe, W.J., 1983: Atmospheric Radiation: 1975-1983. Reviews of Geophysics and Space Physics, 21, 977-1021.

Wiscombe, W.J., and J.W. Evans, 1977: Exponential-Sum Fitting of Radiative Transmission. J. Comput. Phys., 24, 416-444.

Wiscombe, W.J., and G.W. Grams, 1976: The Backscattered Fraction in Two-Stream Approximations. J. Atmos. Sci., 33, 2440-2451.

BOOKS

Chandrasekhar, S., 1960: <u>Radiative Transfer</u>. Dover Publications, Inc., 393 pp.

Goody, R.M., 1964: <u>Atmospheric Radiation</u>. Oxford at the Claredon Press, 436 pp.

Liou, K., 1980: <u>An Introduction to Atmospheric Radiation</u>. Academic Press, Inc., 392 pp.

McCartney, E.J., 1976: <u>Optics of the Atmosphere</u>. John Wiley & Sons, 437 pp.

Paltridge, G.W., and C.M.R. Platt, 1976: <u>Radiative Processes in Meteorology and Climatology</u>. American Elsevier Publishing Company, Inc., 319 pp.

Press, W.H., B.P. Flannery, S.A. Teukolsky, and W.T. Vetterling, 1986: <u>Numerical Recipes The Art of Scientific Computing</u>. Cambridge University Press, 818 pp.

van de Hulst, H.C., 1957: <u>Light Scattering by Small Particles</u>. Dover Publications, Inc., 446 pp.

Wallace, J.M., and P.V. Hobbs, 1977: <u>Atmospheric Science An Introductory Survey</u>. Academic Press, Inc., 476 pp.

SPECIAL PUBLICATIONS and COMMUNICATIONS

Elterman, L., 1970: Vertical Attenuation Model with Eight Surface Meteorological Ranges 2 to 13 km. <u>Air Force Cambridge Research Laboratory</u>, AFCRL-70-0200, Air Force Cambridge Research Laboratory, Cambridge, Massachusetts.

Elterman, L., 1968: UV, Visible, and IR Attenuation for Altitudes to 50 km. <u>Air Force Cambridge Research Laboratory</u>, AFCRL-68-0153, Air Force Cambridge Research Laboratory, Cambridge, Massachusetts.

Isaacs, R.G., W.C-. Wang, R.D. Worsham, and S. Goldenberg, 1986: Multiple Scattering Treatment for Use in the LOWTRAN and Fascode Models. <u>Air Force Geophysics Laboratory</u>, AFGL-TR-86-0073, Air Force Geophysics Laboratory and Atmospheric and Environmental Research, Inc., Cambridge, Massachusetts.

Kneizys, F.X., E.P. Shettle, W.O. Gallery, J.H. Chetwynd Jr., L.W. Abreu, J.E.A. Selby, S.A. Clough, and R.W. Fenn, 1983: Atmospheric Transmittance/Radiance: Computer Code LOWTRAN 6. <u>Air Force Geophysics Laboratory</u>, AFGL-TR-83-0187, Air Force Geophysics Laboratory, Optical Physics

Division, Hanscom AFB, Massachusetts.

Lenoble, J., ed., 1977: Standard Procedures to Compute Atmospheric Radiative Transfer in a Scattering Atmosphere. IAMAP, NCAR, Boulder, Colorado.

McClatchey, R.A., R.W. Fenn, J.E.A. Selby, F.E. Volz, and J.S. Garing, 1972: Optical Properties of the Atmosphere (Third Edition). Air Force Cambridge Research Laboratory, AFCRL-72-0497, Air Force Cambridge Research Laboratory, Hanscom Field, Massachusetts.

Pallmann, A.J., 1988: Thesis Guidance Meetings, 1988-1989. Private Communication St. Louis University, St Louis, Missouri.

Shettle, E.P., and R.W. Fenn, 1979: Models for the Aerosols of the Lower Atmosphere and the Effects of Humididty Variations on Their Optical Properties. Air Force Geophysics Laboratory, AFGL-TR-79-0214, Optical Physics Division, Air Force Geophysics Laboratory, Hanscom AFB, Massachusetts.

Viskanta, R., and T.L. Weirich, 1979: Effects of Pollutants and Urban Parameters on Atmospheric Dispersion and Temperature. Environmental Sciences Research Laboratory, EPA-600/4-79-012, U.S. F...ironmental Protection Agency; Research Triangle Park, North Carolina.

Wiscombe, W.J., 1977: The Delta-Eddington Approximation for a Vertically Inhomogeneous Atmosphere. NCAR Technical Note, NCAR/TN-121, Atmospheric Analysis and Prediction Division National Center for Atmospheric Research; Boulder, Colorado.

VITA AUCTORIS

Spencer Raymond Chapman ███████████████████████

████████████████ He gratuated from Immaculate Conception High
School, Elmhurst, Illinois in June of 1969. He enlisted in the
United States Air Force in October of 1975 as an air defense
radar operator. In 1980 he cross trained into the weather
career field with a follow-on assignment to Offutt AFB,
Nebraska. There, he attented Creighton University and gra-
duated Magnum cum Laude in December of 1984 with a Bachelor of
Science Degree in Atmospheric Science. He was commissioned a
Second Lieutenant in the United States Air Force upon gradua-
tion from Officer Training School in San Antonio, Texas on
April 5, 1985. He was accepted into the Graduate School of
Saint Louis University in the fall of 1987.